Faculty of Engineering and Technology

Joint Master Program in Electrical Engineering (JMEE)

Master Thesis

Online Fault Tolerant Control of Sensor Faults of Wind Turbine

Prepared by:

Moataz G. Sattouf (1185107)

Supervised by:

Dr. Ali Abdo

Dr. Hakam Shehadeh

This Master Thesis is submitted in partial fulfillment of the requirement for the Master Degree in Electrical Engineering

BIRZEIT

July 2022

Online Fault Tolerant Control of Sensor Faults of Wind Turbine

تقنية المتحكم المتسامح الآني والمتزامن لأخطاء المستشعرات في توربينات الرياح

Submitted by:

Moataz Ghannam Sattouf

Approved by the Examining Committee

Dr. Ali Abdo

……

Dr. Hakam Shehadeh

……

Dr. Jamal Siam

……

Dr. Abadalkarim Awad

……

BIRZEIT, PALESTINE
July 2022

Declaration

I declare that this thesis entitled “Online Fault Tolerant Control of Sensor Faults of Wind Turbine” is the result of my own research except as cited in the references. It is being submitted to the master’s degree in Electrical Engineering from the Faculty of Engineering and Technology at Birzeit University, Palestine. The thesis has not been accepted for any degree and is not concurrently submitted in candidature of any other degree.

Name: Moataz G. Sattouf

Signature: …….

Faculty of Engineering and Technology

Joint Master Program in Electrical Engineering (JMEE)

Master Thesis

Online Fault Tolerant Control of Sensor Faults of Wind Turbine

Prepared by:

Moataz G. Sattouf (1185107)

Supervised by:

Dr. Ali Abdo

Dr. Hakam Shehadeh

This Master Thesis is submitted in partial fulfillment of the requirement for the Master Degree in Electrical Engineering

BIRZEIT

July 2022

المستخلص

تعد الضوابط التي تتحمل الأخطاء في مصادر الطاقة المتجددة مجال بحث قوي واتجاه مستقبلي في الطاقة والتحكم الآلي. لذلك، يميل اقتراح البحث هذا إلى تحسين المراقبة والتشخيص والتحكم في توربينات الرياح من خلال تطوير تقنية الفحص الاني والمتزامن للتحكم في الأخطاء في أعطال أجهزة الاستشعار الموجودة في التوربينات الهوائية. توربينات الرياح نظام مكلف ويتم تصنيعه ليعمل لعشرات السنين. لذلك تطلب السلطات والشركات المشغلة السلامة والموثوقية العالية في عمل توربينات الرياح. تتمثل الفكرة الرئيسية لهذا الاقتراح البحثي في التغلب على إشارات القياس المفقودة من المستشعرات وتزويد وحدة التحكم بحلول بديلة لمواصلة تشغيل التوربين لضمان عدم وجود خطر يؤدي لتدمير وتلف لهذا التوربين. في هذا البحث، تتم دراسة ما يسمى بالمنهجيات القائمة على البيانات أو القائمة على الإشارة، والتي تعتمد على تحليل الإشارات المتولدة مباشرة من النظام المرصود. تم اختبار الخوارزمية المطورة والتحقق منها باستخدام Matlab / Simulink استنادًا إلى بيانات وقياسات توربينات الرياح الحقيقية التي تم جمعها للبحث والتطوير في تشغيل توربينات الرياح.

Abstract

Fault-tolerant controls on renewable energy sources are a hot research domain and the future trend in energy and automatic control. Therefore, this research proposal tends to improve the monitoring, diagnosis, and control of the wind turbine by developing an online technique of fault-tolerant control in existing sensor faults in the wind turbine. A wind turbine is an expensive system, and it is manufactured to operate for tens of years. The safety and reliability of the wind turbine are requested by authorities and operated companies. The main idea of this research proposal is to overcome the missing measurement signals of the sensors and provide the controller with alternative solutions to continue the operation of the turbine since there is no risk of damage to this turbine. The developed algorithm has been tested and verified using Matlab/Simulink based on real wind turbine data and measurements collected for research and development of wind turbine operation.

Table of Contents

List of Figures

List of Tables

List of Symbols

v_w	The Wind Speed Acting on The Turbine Blades.
τ_w	The Torque from The Wind Acting on The Turbine Blades
τ_r	The Rotor Torque
ω_r	The Rotational Speed of The Rotor
τ_g	The Generator Torque
ω_g	The Rotational Speed of The Generator
β_r	The Reference to The Pitch Position
β_m	The Measured Pitch Position
$\tau_{w,m}$	An Estimated Wind Torque Based on Wind Speed Measurement
$\omega_{r,m}$	The Measured Rotational Speed of The Rotor
$\omega_{g,m}$	The Measured Rotational Speed of The Generator
$\tau_{g,m}$	The Measured Generator Torque**.**
$\tau_{g,r}$	The Torque Reference to The Generator
P_r	The Power Reference to The Wind Turbine
P_g	The Power Produced by The Generator
$P_{g,m}$	The Measured Power Produced by The Generator
η_g	The Efficiency of The Generator.
η_{gc}	The Efficiency of The Generator and Converter
η_{dt}	The Efficiency of The Drive Train
α_{gc}	The Generator and Converter Model Parameter
λ	Tip Speed Ratio**.**
ζ	The Damping Factor
ω_n	The Natural Frequency
ω_{n2} and ζ_2	The Two Transfer Function Parameters for The Pressure Drop Case
ω_{n3} and ζ_3	The Two Parameters for The Increased Air Content Model
R	Radius of the Blades
C_p	Power Coefficient of The Turbine
C_{Pmax}	The Maximum Value of The Power Coefficient.
C_q	Torque Coefficient of The Turbine
ρ	The Air Density
A	The Area Swept by The Turbine Blades.
m	The Mean Value of The Noise
σ	The Variance of The Noise
n	Sample No
N	The No. Of Samples

Chapter One

Introduction

1.1 Wind power and wind turbines

Technology rapid development has raised power requirement to run the electrical equipment. This put more pressure on fossil fuels and raised energy cost. That is why renewable energy sources must be focused, especially that fossil fuels are extremely limited. In addition to that, it has become a necessity to preserve ecological system and atmosphere from pollution resulting from fossil fuels and greenhouse gases.

Among the most important renewable energy resources comes the wind energy which achieved marvelous results and has attracted the energy investors' eyes. So, it has obtained description "The world's fastest growing renewable energy resource", having achieved 30% average annual growth over the past 20 years. Figure (1.1) exhibits the international wind power capacity over the last 25 years [1,2].

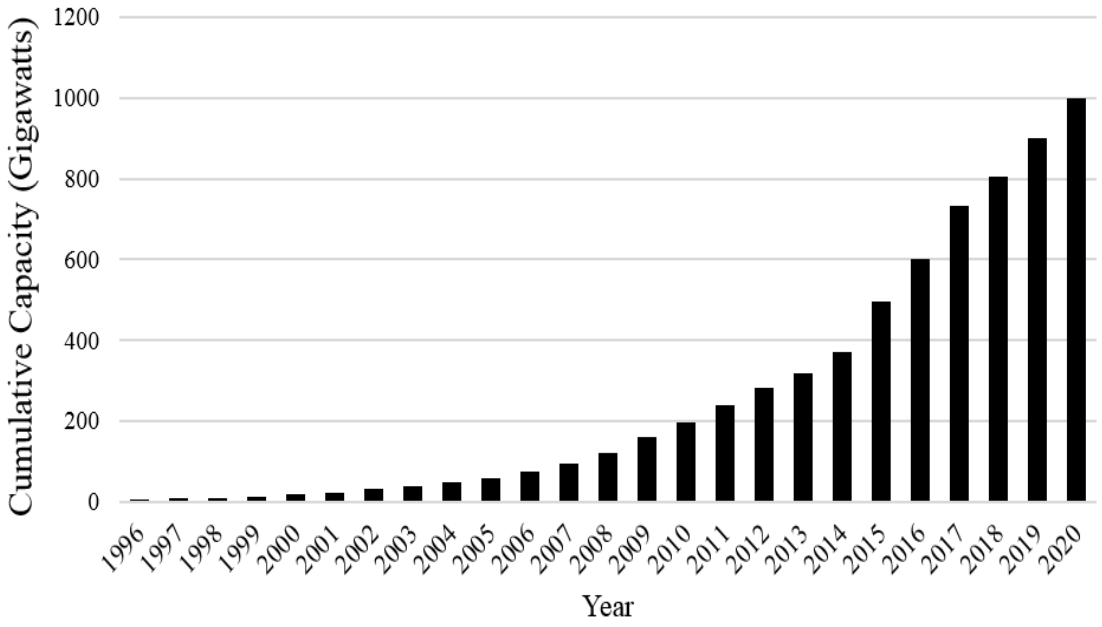

Figure 1.1: World's capacity of wind-generated power [1,2].

Table 1-1 shows the wind power share from the total power requirement for a few countries, whereas table 1-2 shows the development of wind turbines capacity during the last four decades.

Table 1-1: Wind-generated power share of total power production of a few countries.

Country	Wind-generated power percentage	Expected year	Reference
United States	30% (300 GW)	2030	[3]
European Union	12-14%	2020	[4,5]
	25%	2030	
China	15%	2020	[1,4]
Denmark	50%	2020	[6]

Table 1-2: The increase in wind turbines dimensions and ratings in the past 30 years [1].

Length of Impeller Blade (m)	Height of the Holding Tower (m)	Nominal power rating (kW)	Year Applied	Fixation
8.5	30	75	1980-1990	Onshore
15	45	300	1990-1995	Onshore
25	60	750	1995-2000	Onshore
35	70	1500	2000-2005	Onshore
40	95	1800	2005-2010	Onshore
50	100	3000	2010-2015	Onshore
62.5	130	5000	2010-2015	Offshore
75	160	10000	2015-present	Onshore
125	220	20000	2015-present	Offshore

Extensive need for maintenance of these turbines has double down sides; more cost, plus reduction of power generation because of off-time. [7,8]. Therefore, this raises the money spent per energy unit, and consequently power generated from wind turbine might be less viable when it is compared to fossil resources. For instance, offshore wind turbines need maintenance that consumes 20-25% of the entire revenue [9-11] and onshore ones cost 10-15% for 20 years of operation [12].

More maintenance leads to double negative impact, i.e., more maintenance expenses and also, less generated power because of increased off-time [7, 8]. So, the cost of the energy

generated is raised in general and, accordingly, the wind turbine generated power could be less competitive when it is compared to traditional energy resources.

The desired goal in this field is to reduce maintenance cost, decrease downtime, raise the generated power, and therefore develop viability and efficiency [13].

To achieve this goal, Fault Detection and Isolation (FDI) as well as Fault Tolerant Control (FTC) are efficient methodologies. Fault data collected by FDI units can be utilized for optimizing the maintenance process via remote inspection [14]. Using FTC gives equipment chance to achieve the desired sturdiness in terms of faults and, consequently, it can stabilize the wind turbine work at a specified level, in spite of faults availability. This means that the repair requirement and off-time are reduced, the integrity of power generation process grew, and total cost is kept as low as possible [15,16].

Majority of the research and work in this field were stimulated by the rivalry between KK-electronic a/c (its name is changed to "KK-Wind Solutions") and Math Works companies in the period between 2009 and 2015.

Recently, two structures for modelling wind turbine were introduced, inclosing LPV (Linear Parameter Varying) and vague T-S (Takagi – Sugeno) prototypes. It must be kept in mind that many reliable modelling packages for wind turbines are already there like FAST (Fatigue, structure, Aerodynamics and Turbulence) which was designed and built by NREL [17] and the 4.8 MW wind turbine model built by KK-electronic (KK-Wind Solution) by collaboration with Aalborg University [18].

1.2 Fault-Tolerant Control and Fault Diagnosis

Terminology is to be elaborated in the following lines:

- **Fault**: "An unpermitted deviation of at least one characteristic property or parameter of the system from the acceptable / usual / standard condition."

  The difference between fault and failure can be drawn from below definition:
- **Failure**: "A permanent interruption of a system's ability to perform a required function under specified operating conditions."

  Hence, error can be considered a variation of fault, and is defined:
- **Error**: "A deviation between a measured or computed value (of an output variable) and the true, specified or theoretically correct value."

All the above may happen in a technical system. A failure usually causes system shutdown, except if the failure is not in a critical system part.

Faults, like failures, could be critical or non-critical. For example, 20% offset fault in wind measurement is not a severe fault, not like the same amount in pitch actuator.

- **Fault detection**: "Determination of the faults present in a system and the time of detection"
- **Fault isolation**: "Determination of the kind, location and time of detection of a fault. Follows fault detection."
- **Fault identification**: "Determination of the size and time-variant behaviour of a fault. Follows fault isolation."
- **Fault diagnosis**: "Determination of the kind, size, location and time of detection of a fault. Follows fault detection. Includes fault isolation and identification."

Fault detection turns out to be simplest yield, and that is not adequate, mostly fault isolation is required.

Faults might be (non-critical faults) that don't shut down the system or shutting the system off (critical faults). Advanced fault processing involves fault-tolerant techniques. Fault detection and isolation could be enough, but some other techniques may need its amount as well [19]. Fault direct reconstruction is the most important data in FTC. Full fault diagnosis includes decision making stage, if there is a fault, and what its kind is, and what response is.

When fault is reconstructed, new parameters can make the system work well, but they may be needed to be reconfigured back to the original.

For this purpose, a simple fault compensation approach is applied by subtracting the reconstructed faults taken from either the (faulty) inputs or outputs, i.e.

$$u_{corr} = u - \hat{f}_a, \quad y_{corr} = (y + f_s) - \hat{f}_s \tag{1.1}$$

As u and y denote the input and output vector, respectively. f_a and f_s denote the actuator and sensor faults, respectively.

Above corrected inputs and outputs which work as virtual actuators and sensors, respectively, in a way that the original controller can still be used. This is a pragmatic method that doesn't need extra or integrated design of the FTC.

The fault compensation in (1.1) is a strategy of no feedback usually, but it can have feedback that contrasts actual output to referential system which has no faults, and even defining this condition is unclear mostly.

Fault diagnosis and fault tolerant control have many advantages [20]:

- Avoid failures and faults damaging turbine parts by timely detection.
- Reduce service costs by preventing functional parts replacement, by applying incident-based service instead of periodical service.
- Give remote diagnosis details to service teams.
- Increase power generation as fault doesn't stop turbine.

An additional benefit is that, fault diagnosis gives operational advantages because it provides early capture of the fault, and this can make wind turbine safer and less costly.

1.3 Motivation and Goal

The wind turbine is a bulk power producer and needs large investment. Therefore, it should continue its operation despite the faults occurred at different operating conditions. Introduce an algorithm for (online/real-time) fault-tolerant control (AFTC) is a big challenge to detect, isolate and accommodate the fault/s in real-time to enable the wind turbine to overcome the occurred fault/s and continue its operation. Controlling the effects of the fault accommodation process on the performance level and the stability of the wind turbine is a big challenge too.

1.4 Importance and Expected Impact

System monitoring and fault-tolerant control is a promising subject for research. The proposed scheme in this research will contribute to this field of research. The expected impact of this research will lead to:

1. Develop a new FTC algorithm to analyze the sensor faults and design a fault-tolerant monitoring and supervision system for the wind turbine.
2. Increase the reliability of the wind turbines: sending an alternative/estimated signal to the controller to enable the turbine to continue its operation with a small effect on performance level despite the occurred fault/s.
3. Predict the sensors' faults in the wind turbine.

4. Reduce the maintenance cost and the downtime of the turbine.

1.5 Methodology

The Methodology of this research can be summarized as follows:

- Study the wind turbine benchmark model.
- Investigate the sensors and their faults on the operation of the wind turbines.
- Applying a diagnosis technique, known fault detection and isolation (FDI) scheme will be used in the FDI module to detect and isolate the occurred fault/s during system (wind turbine) operation.
- Introduce an online reconfiguration mechanism to accommodate the missing/faulty signals from sensors.
- Test the proposed solution based on real data of the wind turbine using the Matlab/Simulink model.

1.6 Outcomes and Deliverables

The following results are expected at the end of this research:

- Suggest a new approach for online fault-tolerant control, which has a realistic application in wind turbines.
- Reduce some measurement components in wind turbine. The recommended FTC approach is able to substitute the redundant sensors signal with estimated ones.
- Improve safety and reliability of the wind turbines, via achieving a high FTC operation.

Chapter Two

Literature Review

2.1 General Review

Renewable energy sources have received large attention in the last decades due to the pollution effects and limited fuel resources. Wind turbines operate as a generator, which convert wind kinetic energy into mechanical energy through a rotating shaft with three pitch-controlled blades. A distinct motor called pitch motor adjusts each blade pitch angle, i.e., wind turbine has three pitch motors. Yaw motor is used to rotate the shaft horizontally (around the vertical axis) according to the wind direction. The rotating shaft transmits mechanical energy to a generator through a gearbox. The generator is followed by a converter and high voltage transformer to transmit the produced electrical energy to the grid [18].

Fault-Tolerant Control (FTC) schemes are used to accommodate fault/s occurred in the system components during operation and maintains the system's stability with acceptable degradation in the system's performance. FTC schemes are classified into active (AFTC) and passive (PFTC) schemes.

The AFTC scheme has two essential components plus the controller. These components are, a fault detection and isolation (FDI) module and a reconfiguration mechanism, as shown in Figure 2.1. The role of the FDI is to discover and isolate the faults that occurs at different operating conditions and in different system's components. The reconfiguration mechanism - in turn- tries to accommodate the fault/s and send an accommodated signal to the controller for the system to continue its operation regardless of the fault/s with a small effect on the system's performance level.

The main disadvantage of AFTC schemes that their time response may be slow due to large computational processes especially with many simultaneous different and distributed faults. This drawback presents a challenge since a slow time response may impact the stability and reliability of system to be controlled.

Since AFTC’s do control as per condition, they have algorithm to capture the status of the system. In fact, AFTC’s senses, isolates, and assesses the fault. Active fault detection sends extra signals to facilitate or enable fault detection. Fault isolation determines which part malfunctions and that is important to accommodate fault. Faults do not necessarily switch the

part off, and some of them are in a medium stage so they must be evaluated. Faults are either abrupt or incipient. An abrupt fault is detectable easily but it is more severe.

PFTC schemes are offline fault detectors to accommodate only fixed predefined fault. Therefore, they have neither an FDI module nor a reconfiguration mechanism. Unlike AFTC, PFTC schemes are simple, fast, and have no time delay. They are also, flexible to a particular group of faults. In a sense, that the same controller is used either if there is or there isn't a fault. In the design of PFTC's, several performance measures are programmed for cases of fault and no-fault [21].

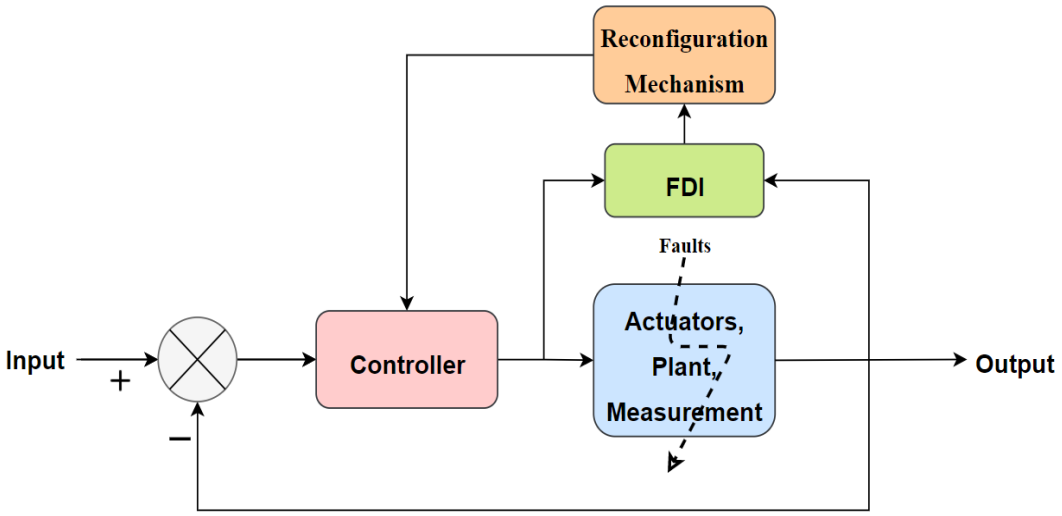

Figure 2.1: AFTC Structure [22].

2.2 Fault Detection and Isolation

There are so many methods for faults' detection. The broadest categorization is into signal-based and model-based methods. Signal-based are the only applicable methods when outputs measurement is done without measuring inputs. They include, for instance, periodic signals analysis (like maximum-entropy assessment) and machines vibrational analysis [23].

On the other hand, model-based measures inputs and outputs, considering standard reference for model-based fault discovery and isolation (FDI) methods [24].

Parameter estimation can be done using identification methods, also a data base can be established to compare system current behavior with the fault-free zone. However, fault identification and isolation are not always possible; a common technique is the least-squares parameter estimation [25].

Majority of model-based FDI methods depend on residuals calculation and evaluation which are defined as “the quantities that represent inconsistency between the actual system’s variables and the mathematical model’s" and "the respond to faults in distinguishing methods" [24].

2.3 Fault Identification / Reconstruction

Typically, Unknown Input Observers (UIO’s) are used for generating residuals but not direct fault estimates. In contrast, [26] introduced a special UIO for direct fault reconstruction, which gives excellent outcomes and depends on only one observer, unlike many other approaches that need an observers’ bank for different faults. Powerful existence conditions should be met for the proposed UIO.

Another way of fault reconstruction is sliding mode observers [27-29]. It is a nonlinear technique used for observers as well as controllers. Its nonlinear switching term can keep motion on sliding surface [30].

For sliding mode observers, the equivalent output injection signal, which outlines the average operation of the switching term, can be estimated to result direct fault estimates. When compared, it is discovered that the sliding mode observer (SMO) works better than UIO when parametric uncertainty is there in the simulation, entailing that the robustness characteristics of the SMO are better. Moreover, SMO needs less strong needs structurally.

SMO observer is best suited for linear systems, since nonlinear switching term only handles faults. For a highly nonlinear model like a wind turbine, a structure like the SMO doesn’t work properly, since sliding term catches nonlinear dynamics and system faults.

As a result, a nonlinear extension of the SMO was added (using Takagi-Sugeno method). Thus, TS structure handles dynamics, and switching term handles faults.

Because of switching term limitations, neither the SMO nor the TS SMO introduced in [31] can simultaneously reconstruct faults which have greatly varying order amount. An adjusted switching term for the TS SMO was proposed in [32].

2.4 Fault-Tolerant Control

There are many different approaches to construct FTC. Those can be categorized into passive (PFTC) and active categories (AFTC). PFTC is built to achieve a certain performance

and to tolerate a certain class of faults, but its range is limited and it operates below optimization in fault-free case [33].

The FTC strategy is formed of two merged steps. The first one is fault detection and isolation (FDI), and the second one is the reconfiguration of the controller to befit fault in the process. The operation and stability of the FTC schemes rely on the precision and preparedness of the fault diagnosis technique in action.

Consequentially, FTC can be applied in the case of fault to secure safe operation. FDI can be done by many methods which had a lot of improvements in the last two decades.

There were a lot of research that was directed to the model and the observer-based fault diagnosis technique. [14,18, 22, 34-43].

2.5 Existing Fault Diagnosis and FTC Methods

FTC avoids components failure from expanding to full system. Nevertheless, it passes some low performance conditions. For designing a PFTC, a satisfying behavior for the nominal control system must be accomplished as an elegant deterioration is permitted when fault is there. In [21], by creating dependence on two controllers. One controller output nothing as the control system senses nominal operation, and the second controller is equal to the nominal one. In the case of a fault, the first one works giving a signal to alter the control system. Other methods, as in [44], depend on a multi-objective control system.

In an AFTC system, a fault diagnosis system is constructed. This needs a residual generator sensitive to internal faults not to changes coming from ambience. This can be done by parity space approaches where residual is decoupled from outside disturbance.

One more way is to design a change detection algorithm, e.g., based on a CUSUM test, capable to spot a variance in signal mean value. Besides, Kalman filter methods can be applied by producing a description of the fault turn into part of the system model, and assessing the fault. Once the fault has been inspected; the AFTC is reconfigured. This might be to reconfigure the controller to depend on estimates in place of measurements. The AFTC system is reconfigured using supervisor, which picks one sensor from many, depending on fault sort [20].

2.6 Fault Diagnosis and Fault-Tolerant Control of Wind Turbines

Here, the current states of fault diagnosis and FTC of wind turbines are reviewed, by going through the literature in hand. Today, wind turbines have sensors for conditions and faults detection. The obtained data may then be used in predicting maintenance time. However, most monitoring systems use signals and vibration analysis in detection. [45].

In matter fact, only a small number of model-based fault diagnosis methods are applied for wind turbines; for example, fault diagnosis systems for pitch sensors and pitch actuators [46,47]. These diagnosis approaches evaluate parameters in the pitch system, and record if a fault has happened using these evaluations. The commonly used way is to distribute condition monitoring systems and turn off the wind turbine if a fault is detected. Anyway, in a few conditions ideas about fault naturalization have been introduced, but not examined or simulated.

During last few decades, advanced FDI procedures for actuator and sensor faults were successfully executed in wind turbine simulation studies. In [84], blade root moment sensor faults and pitch actuator stuck faults can be sensed through robust H∞/H− observer. Fault amounts are then evaluated with a dynamical filter. For examining algorithms work, a linearized simulation model is applied.

Bigger turbine sizes impose the need for redundancy in the components and the sensors for safety. An instance is the pitch system for manipulating rotor blade angle. For every blade in 3-blade rotor, separate pitch system is applied, so that is worst failure condition in pitch system, the other one or two would still have the ability to shut-off turbine.

Adhering to extra safety provisions, redundancies entail extra expenses and probably more turbine off-time due to faults in the redundant parts. The increase in safety may thus mean a loss of energy production and profit. One possible solution is to invest in functional redundancies instead of hardware ones. Even when we decrease hardware redundancies, big size wind turbines are exposed to faults due to several reasons. Currently, many of these faults often cause turbine shutdowns, because of safety issues. Particularly in offshore wind turbines, this might force operator to accept the fact that some of the turbines are deactivated since access to them is very difficult due to harsh weather conditions.

The continuous need for consistent power generation imposes need for integral fault diagnosis and FTC systems that keep the turbine running even when faults are there, probably

at less velocity, and simultaneously handling the rectification. Beside raising availability and declining turbine shut down time, intelligent fault diagnosis schemes could cancel the urge for extra hardware abundance, if virtual sensors may partially substitute redundant hardware sensors.

Complication in modern control systems and algorithms has led to continuous interest in fault diagnosis methods of systems. There have been many challenges in knowing fault diagnosis systems and how they add value to the control systems. There are three classification of fault diagnosis systems: model-based, hardware-based and history-based fault diagnosis systems.

Large control systems are utilized to measure quality, safety, and functional reliability over time. Control systems components decay over time because of wear and interaction with ambience. Accordingly, it is a requirement for control systems to be capable to diagnose and fix faults disregarding their operational mode, either online or offline.

2.7 FDIR and Residual Concept

Fault diagnosis system's main idea is to know the kind, size, and position of the fault, and also determining time of detection, according to the system's measurements. A general scheme of model-based fault diagnosis is shown in Figure 2.2. Fault diagnosis is implemented through two stages: First, a signal called residual is initiated utilizing existent input–output measurements in the diagnosed system. When there are no faults in the system, residual signal is roughly zero, and other measurement values (variant from zero) indicate fault. Residual signal value might be of one fault (scalar) or multiple faults (vector). The type of the residual generator varies from an analytical mathematical model to a black-box model of the system. Decision making is done in the second stage to examine faults behind the residual signals. Furthermore, decision making mechanism ranges from threshold to complex statistical methods [48].

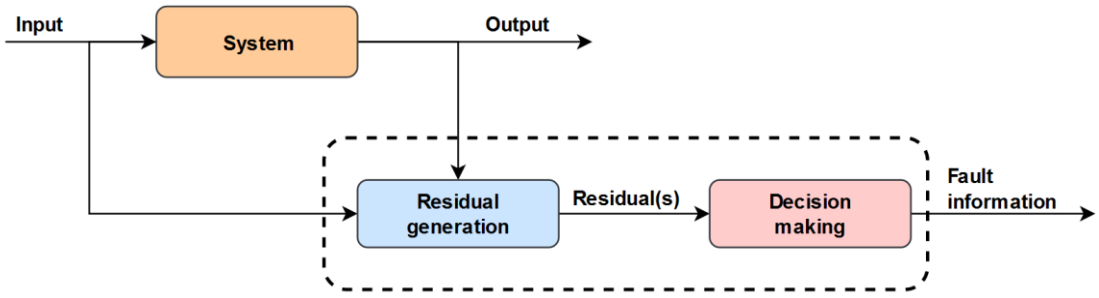

Figure 2.2: General scheme of model-based fault diagnosis [48].

Fault detection, isolation, and reconfiguration (FDIR) is an essential subject in all engineering branches (chemical, aerospace, nuclear . . . etc.). FDIR is, as well, needed in applications built with high redundancy e.g. wind applications, since it is known for reliable and quick fault.

The International Federation of Automatic Control (IFAC), defines “Fault” as an unpermitted deviation of at least one characteristic property or parameter of the system from the acceptable/usual/standard.

Such malfunctions are expected to occur in the individual unit of the plants, sensors, actuators or the switching logic components. When an error occurs FDIR secures safe running of a system when through fault detection and isolation (FDI), and controller reconfiguration is response to fault.

The FDI outcome will be one of two: either that there is some issue also it specifies the location of the fault, or that there is nothing wrong. Generally, FDI methods rely on redundancy, which can take form of a hardware redundancy or analytical redundancy as illustrated in Figure 2.3. The basic concept of hardware redundancy is to compare duplicative signals generated from several hardware, like measuring same signal emitted by two sensors. Amongst several techniques that are commonly used in hardware redundancy approach are the cross-channel monitoring (CCM) method, residual generation using parity generation (depending on sensor geometry or signal pattern), and signal processing methods like wavelet transformation, etc. [39], [49].

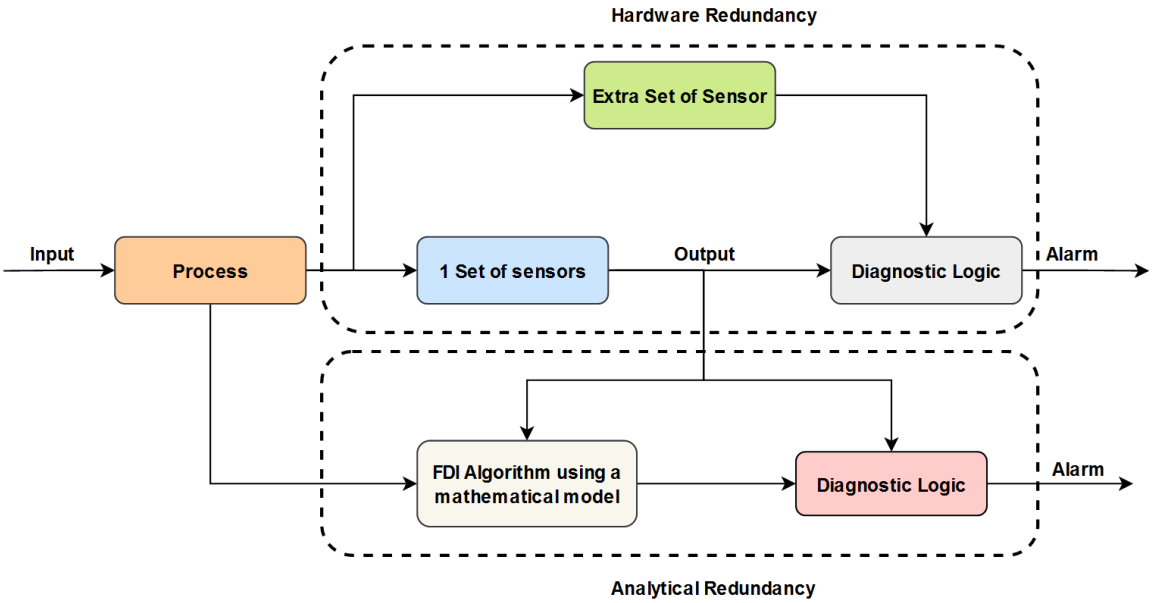

Figure 2.3: Illustration of the concepts of hardware redundancy and analytical redundancy for FDI [49].

Analytical redundancy saves money when compared to hardware redundancy, since it doesn't need adding extra hardware. It, basically, uses a mathematical model of the system along with estimation methods for FDI.

Analytical redundancy can be generally divided into quantitative and qualitative model-based methods. However, making it effective is a more difficult task due to the need to ensure it is robust enough and able to resist noise and disturbances.

The qualitative model-based methods use artificial intelligence (AI) techniques, like pattern recognition, to catch differences between actual behavior and model-predicted one. On the other hand, the quantitative model-based methods use explicit mathematical models and control theories to generate residuals for FDI. The thesis, however, focuses mainly on the quantitative model-based approach of FDIR.

A general structure of an analytical redundancy-based (or model-based) FDIR system is illustrated in Figure 2.4. It consists of three steps: First is to generate a set of variables (residuals) using one or more residual generation filters. Residuals must ideally be roughly zero under ideal conditions (fault-free). To make them practical, they have to be prone to noise, disturbances, and model uncertainties and greatly sensitive to faults. Some FDIR schemes use many residual generation filters in parallel to achieve fault isolation. In these schemes, every filter is designed to be sensitive to a pre-selected set of faults. The second step is to decide if a fault has occurred (fault detection) and on the faults' type (fault isolation). This is done using

statistical tools to check if the residuals have considerably deviated from zero. Finally, the controller is reconfigured online to respond to the detected faults [49].

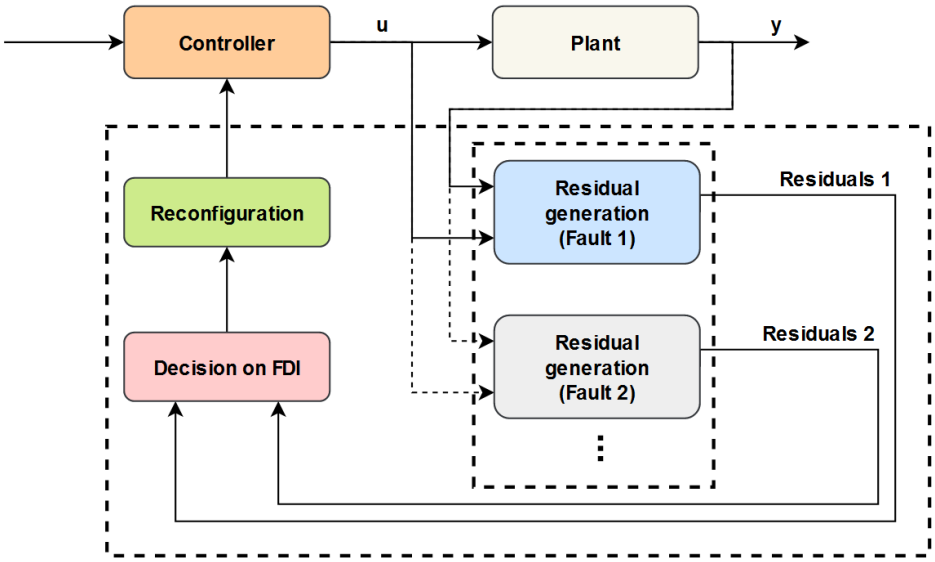

Figure 2.4: Fault detection, isolation, and reconfiguration scheme [49].

Applying analytical redundancy approach, residuals are generated based on a mathematical model of the system. This mathematical model might be developed based on theoretical laws, or empirically based on experience. Practically, it can't describe the system exactly due to errors. In addition, noise in practical systems result in residuals deviating from zero under no-fault conditions.

There are generally two approaches to overcome this problem, shown as follows.

1) Robust Residual Generation: A filter that is immune to noise and able to detect only noises. Examples of this approach are the fault detection filters [50- 55], the observer-based methods [56], [57], the parity relation methods [58], [59], the parameter estimation methods [60], [61], and Kalman filter-based methods [62].

2) Robust Residual Evaluation: A robust algorithm for testing residuals. The strategy relies on robust methods of detecting a change in signals corresponding to faults. The simplest decision rule is to decide a fault occurs when the value of a residual is above a pre-determined threshold. More complex decision rules may contain adaptive thresholds, or may use statistical decision theories like generalized likelihood ratio (GLR) test or sequential probability ratio test (SPRT) [63], [64], [65].

The FDIR problem is a subject on which received significant interest by many authors. [63] Has introduced key concepts of analytical redundancy in model-based FDI. [57] Has presented a comprehensive survey of observer-based FDI methods. [61] Has introduced some basic fault detection methods, and gave examples of fault detections by parameter monitoring and special correlation methods. Many surveys of parity relation methods in FDI can be found in [59], [66] and [67]. Several publications have introduced comprehensive review of the concepts and applications of model-based FDIR methods [65], [68-71]. A three-part review paper [72-74] have concentrated mainly on FDI methods and applications in process chemical engineering. [75] Has reviewed numerical and artificial intelligence FDI methods. [76] Has introduced various model-based FDIR techniques.

A switching fault-tolerant control (SFTC) strategy for a doubly-fed induction generator-based wind turbine (DFIG-WT) subject to rotor and stator current sensor faults is proposed in [77]. A novel stator-current-loop vector control scheme is introduced for the regulation of DFIG-WT without involving rotor currents. This SFTC strategy switches between the rotor and stator current vector controllers via a switching logic based on Kalman filter-based fault detection and isolation (FDI) scheme. [78] Introduced a novel fault-tolerant cooperative control scheme based on an adaptive control reconfiguration approach that is augmented with an innovative control reallocation mechanism in a cooperative framework.

A novel active fault-tolerant control (FTC) methodology for WT, which minimizes the economic cost of WT by achieving the two broad objectives: power maximization and fatigue reduction, possibly under the effect of torque bias faults in converters is proposed in [79]. The proposed FTC system is composed of two modules: fault detection and diagnosis (FDD), and controller reconfiguration (CR). The CR module using a model-predictive control (MPC) technique has been developed, where the primary issue is that the constraint set is not convex in decision variables.

[80] Proposed a reliable load mitigation scheme, referred to as “fault-tolerant individual pitch control,” for individually adjusting the pitch angle of wind turbine blades in the presence of blade pitch actuator faults. [81] Introduced an adaptive sliding mode observer (ASMO)-based approach for wind turbines subject to simultaneous faults in sensors and actuators. This ASMO enables the simultaneous detection of actuator and sensor faults without the need for any redundant hardware components. It also enables the accurate estimation and reconstruction

of the descriptor states and disturbances. Fault tolerance is achieved by implementing a signal correction scheme to recover the nominal behavior.

2.8 Fault Diagnosis Methods Classifications

There is large amount of literature about dynamic systems fault diagnosis. From a modelling point of view, some methods need accurate system models (plants), quantitative models or qualitative models. Anyway, some methods depend just on historic system data. Although fault diagnosis received considerable review, it is noted that classification of fault diagnosis methods mostly is not consistent. The reason is that researchers concentrate on a specific branch, like analytical models, of the big field of fault diagnosis. Figure 2.5 depicts this classification. Fault diagnosis methods are classified into three main categories: model-based, hardware-based and history-based.

A. Model-Based Fault Diagnosis

These methods usually use a model developed based on basic understanding of plant or process physics. They are classified into qualitative or quantitative.

- Qualitative methods.

  Qualitative model-based fault diagnosis is classified into abstraction hierarchy, fault trees, diagraphs and fuzzy systems. These methods utilize a model where the input–output relationship of the plant is expressed in terms of qualitative functions goes around different units in the process.

- Quantitative Methods

  These methods utilize a model where the input– output relationship of the plant is coded in terms of mathematical functions. As shown in Figure 2.5, quantitative model-based fault diagnosis is generally classified into analytical redundancy, parity space, Kalman filter (KF), parameter estimation and diagnostic observers.

B. Diagnostic observers.

In the fault diagnosis literature, different types of diagnostic observers for residual generation can be noticed, including the following:

- Residual generation using Eigen-structure assignment.

  It separates directly the generated residual from disturbance (disturbance may not be separated from state estimation).

- Residual generation using unknown input observer (UIO).

  Its principle is to make the state estimation error decoupled from the unknown inputs (disturbances).

- Residual generation using fault detection filter.

  It is a full-state estimator with a special choice of the feedback gain matrix.

- Residual generation using bilinear observer.

  A special class of non-linear systems can be handled using bilinear observers. They are designed according to two approaches; the first one uses the Lyapunov method, whereas the second approach is uses techniques developed for linear UIOs.

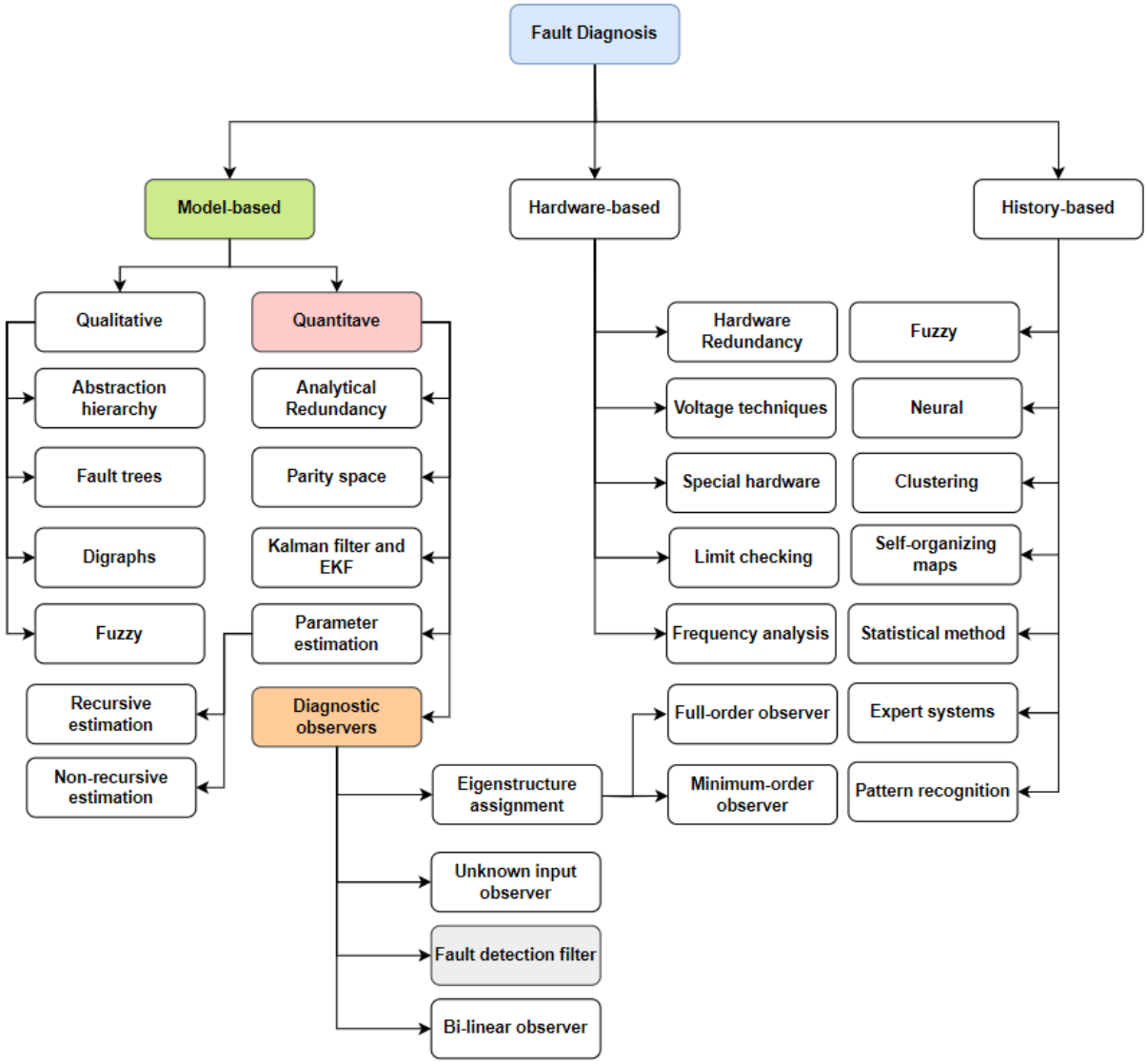

Figure 2.5: Classification of fault diagnosis methods [48].

Analytical redundancy methods for fault detection and identification use a modelled dynamic relationship between system inputs and measured system outputs to form a residual process. Nominally, faults are detected when the residual process is nonzero only when there is a fault which is zero at other times. An example of a residual process for an observable system while there is no noise is the innovations process of any stable linear observer. A detection filter is a linear observer with the gain constructed so that when a fault occurs, the residual responds in a predetermined direction, thus activating simultaneous fault detection and identification.

Identifying the components at risk of failure and then modifying them is very important as the reduction of the incidence of software failure improves reliability. In fact, any violation of reliability will result in intolerable losses to the software system. one of the technologies used to improve the software system's reliability is Software fault tolerance. Software fault tolerance is used to detect an error occurring or has already occurred in the software or hardware in which the software resolves this error according to specifications. The ad-hoc method is based on hardware fault tolerance as the program versions are closely parallel with retrying the same operation in the hope that the problem will be resolved in the next attempt. In other words, software fault tolerance attempts to leverage the experiences to solve other problems. However, doing so produces a need for design variety to build a redundant system properly.

The software carrier is called a module, and the module completes a specific and distinct function. When any module fails in the software system, the solution is to redundancy another module, which can replace the failed module to ensure the consistency of system operation. Therefore, the system with redundant modules will affect the system's performance and enhance the fault tolerance to ensure reliability.

In some applications, the detection filter structure is sensitive to small parameter variations because the eigenvectors of the observer are ill-conditioned.

Detection filters form a class of linear observers that produce residuals with known and fixed directional characteristics in response to a set of design fault directions. Practically, reliable fault isolation works only when the detection space structure is insensitive to system parameter variations. A left-eigenvector assignment approach is developed to allow for the application of existing results relating suprema controllability subspaces and ill-conditioned

eigenvectors. Adjustments to the detection filter structure that produce improved eigenvector conditioning and sensitivity to system parameter variations are applied to an aircraft accelerometer fault detection filter [82].

Chapter Three

Wind Turbine Description

This chapter aims to review wind turbine components studied in the thesis, and to elaborate how to control it to optimize the performance relying on the wind speed. Accordingly, a reference controller is designed following the wind turbine control rules.

3.1 Wind Turbine Components

Wind turbine components are basically introduced in this section. The wind turbine selected here is built by kk-electronic a/s (kk-Wind Solutions) applying Danish perspective, which forms the basis for contemporary turbine designs. Figure 3.1 shows the horizontal axis wind turbine utilizing three-bladed rotor with active yaw system that keeps the rotor directed upwind [83].

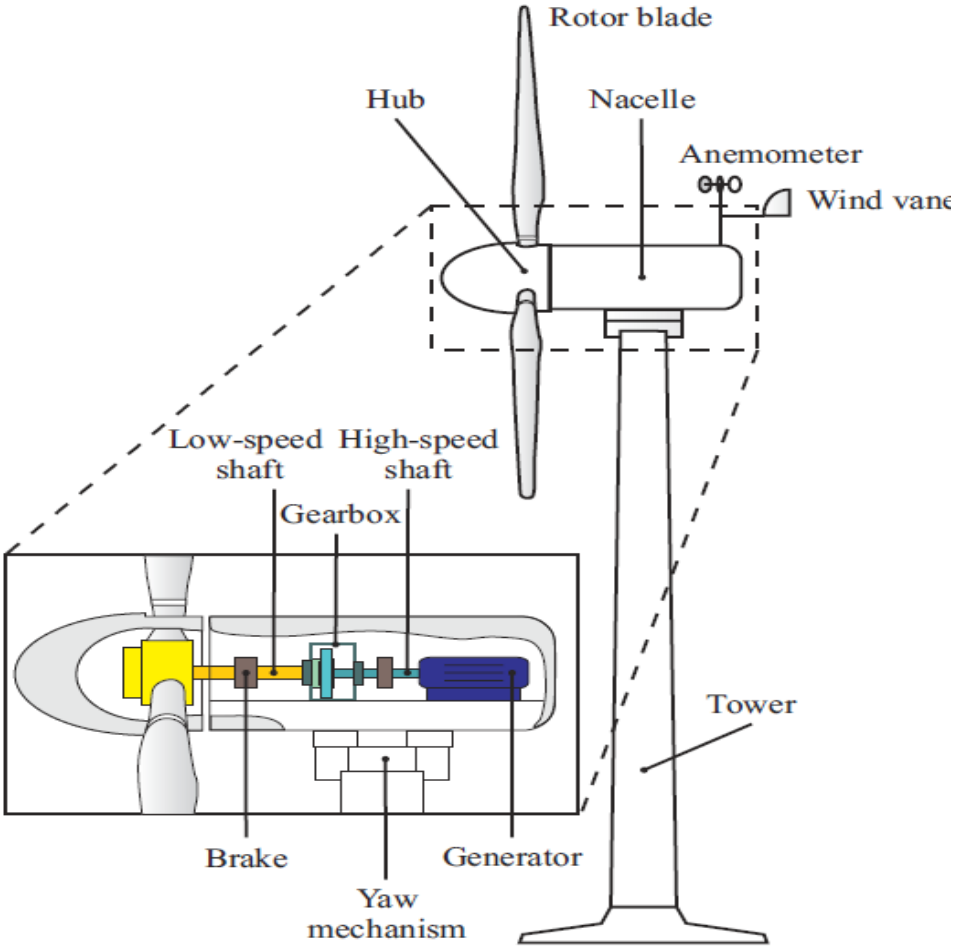

Figure 3.1: Horizontal-axis wind turbine parts and components [20].

The main turbine components can be explained as [20]:

- Anemometer which measures the wind speed. The turbine starts to rotate once speed hits a certain value (lower limit), and stops when it reaches a higher limit (cut-out at high speed).
- Brakes: mechanical, hydraulic or electric and work like car brakes.
- Gearbox: Connects low-speed shaft to high speed one, increasing generator speed to a value that can generate power.
- Generator which converts kinetic rotational energy into electric energy. Its power can reach a maximum of 5 MW.
- High-speed shaft which handles driving generator.
- Hub and rotor blades: The hub link the rotor blades to the low-speed shaft. Pitching the blades is applied to increase the efficiency at low wind speeds and decrease efficiency in high wind speeds to prevent structural damage in the turbine.
- Low-speed shaft which is responsible for connecting the rotor and gearbox.
- Nacelle which is fastened at the top of the tower and it contains the gearbox, low- and high-speed shafts, generator, and brakes.
- Tower which lifts the nacelle and the rotor. Taller tower produces more power because higher wind speeds occur at higher heights.
- Wind vane which gets wind direction to make yaw mechanism able to make turbine normal to wind direction at all times.

Yaw mechanism makes wind turbine blades normal to the wind direction using data from wind vane [84].

3.2 General Control Strategy

Figure 3.2 shows the block diagram of wind turbine benchmark work. The components are shown in boxes. Blades absorb power by aerodynamic forces. Pitch angle is controlled by pitch system and this controls the power obtained. Drive train system links low speed rotor shaft to high-speed generator shaft, transferring the aerodynamic torque from rotor to generator. Generator is induction type having power electronics devices, and it can generate electricity and adjust its characteristics [85].

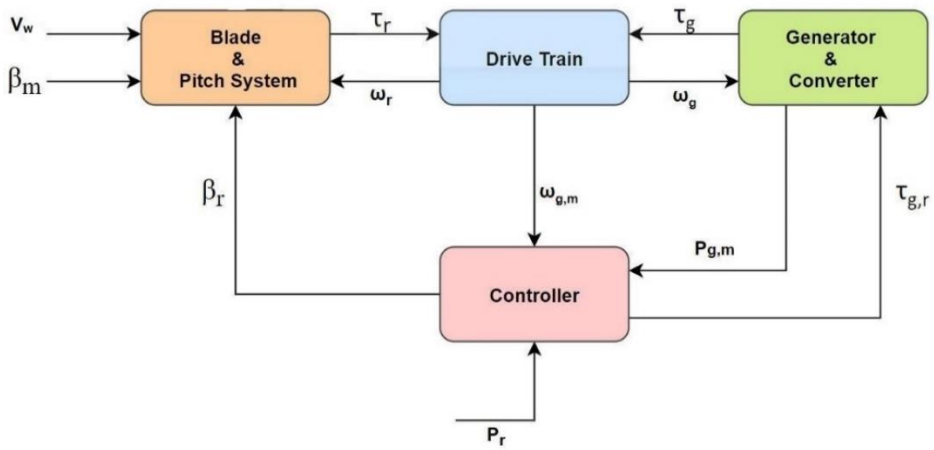

Figure 3.2: Block diagram of control system for wind turbine (Benchmark Model).

This part explains how to control variable-speed, variable-pitch wind turbine along a typical operating trajectory, and to go through control process variables. FTC and FDI actually depend on conditions of the closed-loop system. The control aims to increase power generation and reduce expenses which depend on operation conditions, so the turbine is following a specific trajectory, as shown in Figure 3.3. This trajectory is generated using a control strategy shown in Figure 3.4, exhibiting the control signals and rotor speed for producing the targeted output power. Turbine produces power only in control modes 1 & 2 having limited speeds. Below cut-in there is no generation because it is not feasible, and above cut-out it is stopped to prevent turbine damage [20].

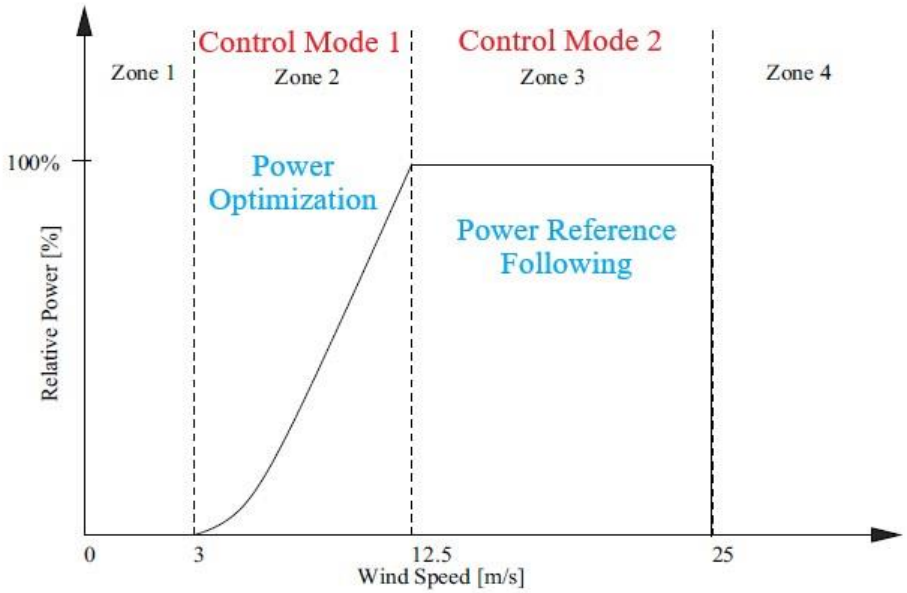

Figure 3.3: Typical power curve for the wind turbine [18].

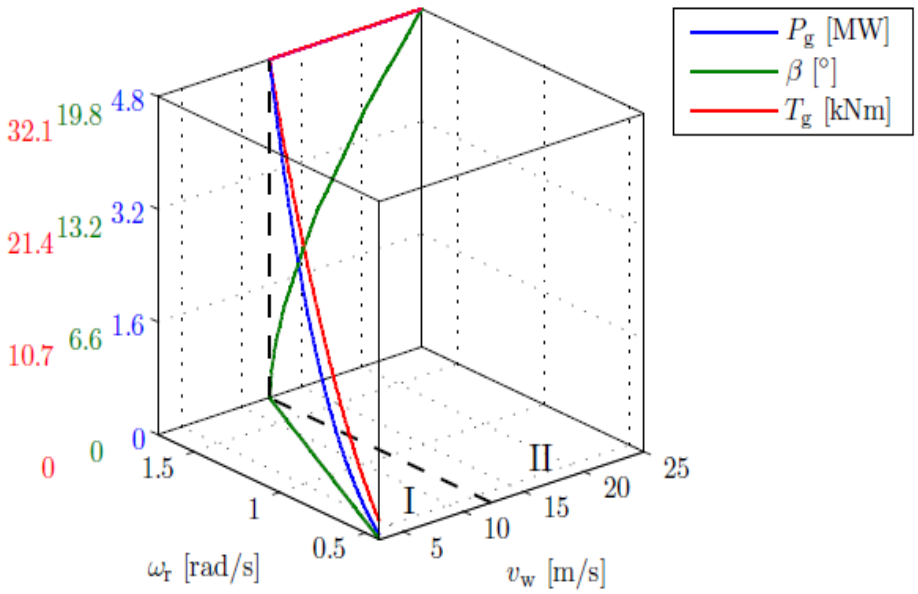

Figure 3.4: Typical control strategy for applying the typical power curve [20].

- **Control Mode 1** is between the cut-in wind speed (3 m/s), and the rated wind speed (12.5 m/s). Power optimization is achieved here by varying the generator torque to optimize it between blade tip speed and wind speed. So, aerodynamics efficiency is maximized.
- **Control Mode 2** is between the rated wind speed, and the cut-out wind speed (25 m/s). It is maintained at rated value to avoid damage and noise. Two separate sets of controllers are used (for two regions) and interconnected by transfer mechanism. Figure 3.5 exhibits a block diagram of a reference controller used to maintain a frame of reference; it complies with kk-electronics.

Reference controller uses two different controllers: one for the partial load region and one for the full load region. At speed below rated, an optimal pitch angle is controlled to optimize tip-speed ratio by controlling the generator torque, i.e., setting the two switches in Figure 3.5 to be in Position I [20].

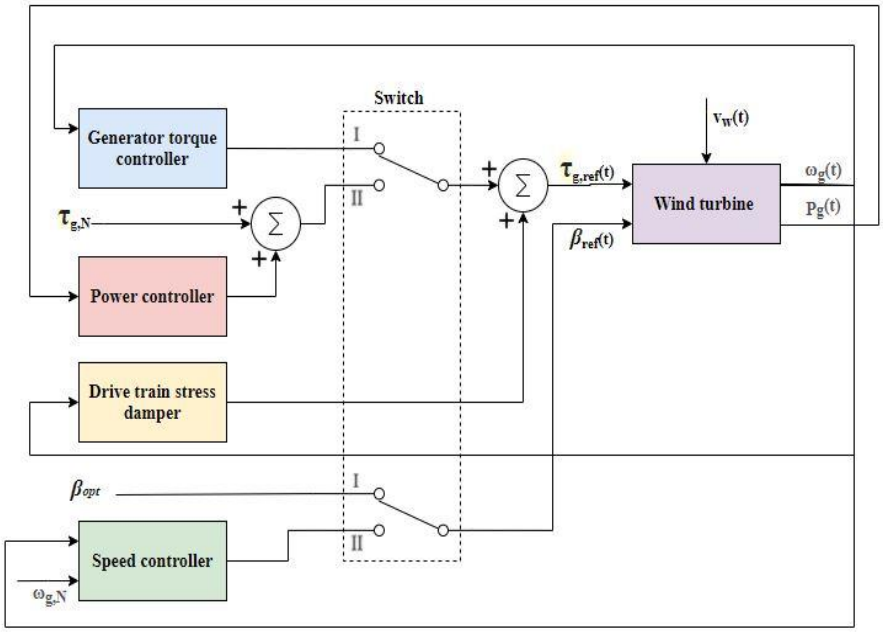

Figure 3.5: Reference controller structure [20].

Above rated speed, output power is maintained at a certain value by pitching the rotor blades, while the power controller function is solving steady-state errors by controlling the generator torque. i.e., setting the two switches in Figure 3.5 to be in Position II. A transfer mechanism is used to jump between the two control zones [20].

3.3 Wind Turbine Parts Modelling

Wind turbine parts models are presented in this section [18].

A. Wind Model

The combined wind (V_W) model is given by:

$$V_w(t) = V_m(t) + V_s(t) + V_{ws}(t) + V_{ts}(t) \quad (3.1)$$

As in the above equation four parts are the main components that wind model consists of, these are:

- $V_m\,(t)$ mean wind (slow wind variations): a set of measured wind data process caused slowly varying wind sequence by using low pass filter.
- $V_s\,(t)$: stochastic part which is modelled by Kaimal filters.
- $V_{ws}\,(t)$ wind shear this happens from wind energy lost at the surface of earth causes wind speed increases as the distance to the earth surface increases, which is given by:

$$v_{ws,i}(t) = \frac{2v_m(t)}{3.R^2}.\left(\frac{R^2.\alpha}{3.H}X + \frac{R^4}{4}.\alpha.\frac{\alpha-1}{2.H^2}.X^2\right) + \frac{2v_m(t)}{3.R^2}.\left(\frac{R^2}{5}.\frac{(\alpha^2-\alpha).(\alpha-2)}{6.H^3}.X^3\right) \quad (3.2)$$

Where:

- $x = \cos\theta_{r^*}(t)$ where θ_{r^*} is the angular position of the three blades as below:
  - $\theta_{r1}(t) = \theta_r(t)$
  - $\theta_{r2}(t) = \theta_r(t) + \frac{2}{3}\pi$
  - $\theta_{r3}(t) = \theta_r(t) + \frac{4}{3}\pi$
- α and H are two aerodynamic parameters.

- $V_{ts}(t)$ tower shadow which is given by:

$$v_{ts,i} = \frac{m.\bar{\theta}_{r,i}(t)}{3.r^2}.(\varphi + v) \quad (3.3)$$

where:

- $\varphi = 2a^2\frac{R^2-r_0^2}{(R^2+r_0^2)sin\left(\left(\bar{\theta}_{r,i}(t)\right)^2+k^2\right)}$
- $v = 2a^2k^2\frac{(r_0^2-R^2)\left(r_0^2\sin\left(\bar{\theta}_{r,i}(t)\right)^2+k^2\right)}{R^2\sin\left(\bar{\theta}_{r,i}(t)\right)^2+k^2}$
- $m = 1 + \frac{\alpha.(\alpha-1).r_0^2}{8.H^2}$
- $\bar{\theta}_{r,i}(t) = \theta_r(t) + \frac{(i-1).2\pi}{3} - floor\left(\frac{\theta_r(t)+\frac{(i-1).2\pi}{3}}{2\pi}\right).2\pi$

  where:
  - The function floor *(x)* is the largest integer not greater than *x*.
  - r_0 is the radius of the blade hub.
  - *k* is an aerodynamic parameter.

B. Blade and Pitch Model

The model is consisting of a combination of two parts, which are:

1. Aerodynamic Model and valid for relatively small deviations between the pitch angles and is given by:

$$\tau_r(t) = \sum_{1\le i\le 3}\frac{\rho\pi R^3 C_q\left(\lambda(t),\beta_i(t)\right)v_{w,i}(t)^2}{6} \quad (3.4)$$

2. Hydraulic Pitch System Model which is a piston servo system modelled by a second-order transfer function and is given by:

$$\frac{\beta(s)}{\beta_r(s)} = \frac{\omega_n^2}{s^2 + 2.\zeta\omega_n.s + \omega_n^2} \tag{3.5}$$

As the pitch references is changed the sensor fault modelled accordingly and is given by the below equation [18]:

$$\beta_{\mathrm{r,f,i}}[n] = \beta_{r,i} - \frac{\Delta\beta_{i,m1}[n] + \Delta\beta_{i,m2}[n]}{2} \tag{3.6}$$

Where $\beta_{\mathrm{r,f,i}}[n]$ is the new pitch reference in which the sensor fault is contained, and $i \in \{1,2,3\}$

C. Drive Train Model

A two-mass drive train model can be used:

$$J_r\dot{\omega}_r(t) = \tau_r(t) - K_{dt}\theta_\Delta(t) - (B_{dt} + B_r)\omega_r(t) + \frac{B_{dt}}{N_g}\omega_g(t) \tag{3.7}$$

$$J_g\dot{\omega}_g(t) = \frac{\eta_{dt}K_{dt}}{N_g}\theta_\Delta(t) + \frac{\eta_{dt}B_{dt}}{N_g}\omega_r(t) - \left(\frac{\eta_{dt}B_{dt}}{N_g^2} + B_g\right)\omega_g(t) - \tau_g(t) \tag{3.8}$$

$$\dot{\theta}_\Delta(t) = \omega_r(t) - \frac{1}{N_g}\omega_g(t) \tag{3.9}$$

Where:

- J_r is the moment of inertia of the low-speed shaft
- K_{dt} is the torsion stiffness of the drive train
- B_{dt} is the torsion damping coefficient of the drive train
- B_g is the viscous friction of the high-speed shaft
- N_g is the gear ratio
- J_g is the moment of inertia of the high-speed shaft
- η_{dt} is the efficiency of the drive train
- $\theta_\Delta(t)$ is the torsion angle of the drive train

D. Generator and Converter Model

The generator and converter are modelled by a first-order transfer function as:

$$\frac{\tau_g(s)}{\tau_{g,r}(s)} = \frac{\alpha_{gc}}{s + \alpha_{gc}} \tag{3.10}$$

where α_{gc} is the generator and converter model parameter.

The generator output power is given by:

$$P_g(t) = \eta_g \omega_g(t) \tau_g(t) \tag{3.11}$$

where η_g is the generator efficiency.

E. Controller

Controller will happen in discrete time with a sample frequency at 100 Hz. Later on, all time dependent variables are indicated as discrete-time variables.

1. The controller starts in mode 1.
2. The control mode switches from mode 1 to 2 if:
   $P_g[n] \geq P_r[n] \vee \omega_g[n] \geq \omega_{nom}$
   where ω_{nom} is the nominal generator speed.
3. The control mode switches from mode 2 to mode 1 if:
   $\omega_g[n] < \omega_{nom} - \omega\Delta$
   where ωΔ is a small offset subtracted from the nominal generator speed to avoid the switching between the two control modes all the time.

- **Control Mode 1:** The reference torque to the converter $\tau_{g,r}$ is as follows:

$$\tau_{g,r}[n] = K_{opt} \left(\frac{\omega_g[n]}{N_g} \right)^2 \tag{3.12}$$

$$K_{opt} = \frac{1}{2} \rho A R^3 \frac{C_{p_{max}}}{\lambda_{opt}^3} \tag{3.13}$$

λ_{opt} is found at the optimum point in the power coefficient (C_p) mapping of the wind turbine. This optimal value is reached by setting the pitch reference to zero ($\beta_r[n] = 0$).

- **Control Mode 2:** The major control actions in this mode is trying to keep $\omega_g[n]$ at ω_{nom}.

$$\beta_r[n] = \beta_r[n-1] + k_p e[n] + \left(k_i * T_S - k_p\right) e[n-1] \tag{3.14}$$

$$e[n] = \omega_g[n] - \omega_{nom} \tag{3.15}$$

The converter reference is used to restrain fast disturbances by

$$\tau_{g,r}[n] = \frac{P_r[n]}{\eta_{gc} * \omega_g[n]} \tag{3.16}$$

F. Sensors

The combination of actual variable value and stochastic noise is used to model each sensor. Mean value and the variance of noise for the various measurements are as follows:

1. m_w, σ_w (wind speed - v_w).
2. m_β, σ_β (pitch angle - β).
3. $m_{\omega r}$, $\sigma_{\omega r}$ (rotor speed – ω_r).
4. $m_{\omega g}$, $\sigma_{\omega g}$ (generator speed – ω_g).
5. $m_{\tau g}$, $\sigma_{\tau g}$ (generator torque – τ_g).
6. m_{Pg}, σ_{Pg} (generator power - P_g).

3.4 Benchmark Model

Several researches have recently tried their FDI methods on the wind turbine benchmark model first introduced in [14] and later described in more detail in [18]. It is a reduced-order model executed in MATLAB/Simulink and it includes a torsional-flexible drivetrain plus delay models for pitch angle and converter dynamics. Unlike other models, degrees of freedom for tower and blades are not there. The benchmark model contains a group of pre-defined actuator and sensor faults plus detection needs [86].

Another feature that is worth listing regarding the reduced-order benchmark model in [14,18] is that a double redundancy is supposed for all sensors (rotor speed, generator speed, pitch angles), and in the sensor fault scenarios just one of the two sensors for one amount is influenced by a fault at a time. This means in case of a fault in one rotor speed measurement, there is one more right rotor speed sensor available, equally for generator speed and pitch angle

measurements. The double sensor redundancy assumption in the benchmark model thus constitutes a considerable indulgence of the FDI demands.

The aerodynamic characteristics of the blade can be measured with $Cp\ (\beta, \lambda)$ – power coefficient, $Cq(\beta, \lambda)$ – torque coefficient and $Ct(\beta, \lambda)$ – thrust coefficient. The mentioned coefficients are functions of β, i.e., blade pitch angle and λ, i.e., tip speed ratio having the formula of $\lambda = R.\frac{\omega_r}{v_\omega}$, where R is blade length (impeller radius), ω_r is blade rotor angular speed and v_ω is the effective wind speed at the rotor plane. These coefficients are usually there as numerical default or retrieval info or empirical formulas for a specific blade profile. Figure 3.6 shows torque coefficient of the benchmark model [18].

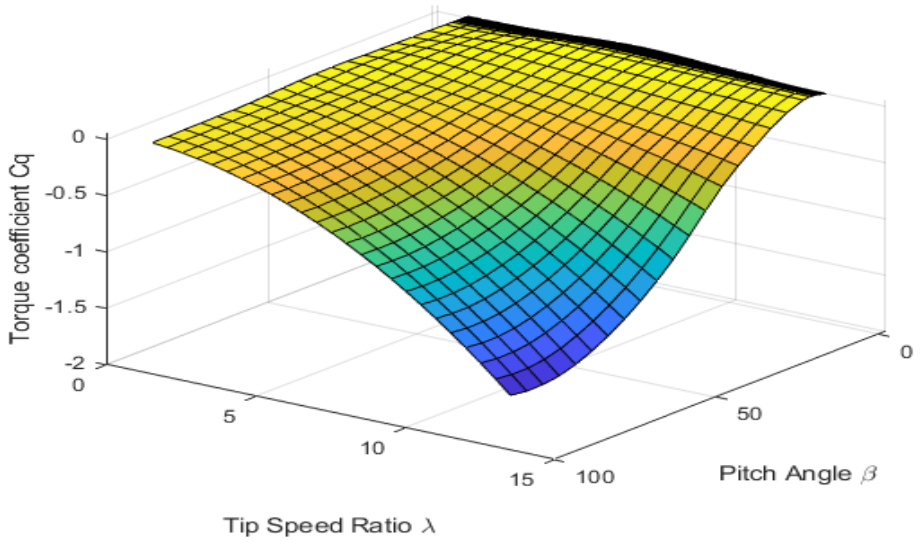

Figure 3.6: Torque coefficient "Cq (β,λ)" of the benchmark model [18].

3.4.1 Model Parameters

The parameters of the benchmark model are listed in tables (3.1-3.6) [18].

Table 3-1: Wind model parameters.

α	H	r_0
0.1	*81 m*	*1.5 m*

Table 3-2: Blade and pitch model parameters.

R	**ρ**	**ζ**	**ω_n**
57.5 m	*1.225* $\frac{kg}{m3}$	*0.6*	*11.11* $\frac{rad}{s}$
ζ_2	**ω_{n2}**	**ζ_3**	**ω_{n3}**
0.45	*5.73* $\frac{rad}{s}$	*0.9*	*3.42* $\frac{rad}{s}$

Table 3-3: Drive train model parameters.

B_{dt}	B_r	B_g	N_g	K_{dt}
$775.49 \frac{Nms}{rad}$	$7.11 \frac{\text{Nms}}{rad}$	$45.6 \frac{\text{Nms}}{rad}$	95	$2.7.\ 10^9 \frac{Nm}{rad}$
η_{dt}	η_{dt2}	J_g	J_r	
0.97	0.92	390 kg. m^2	$55.\ 10^6$ kg. m^2	

Table 3-4: Generator and Converter model parameters.

α_{gc}	η_{gc}
$50 \frac{\text{rad}}{s}$	0.98

Table 3-5: Controller parameters.

K_{opt}	K_i	K_p	ω_{nom}	ω_Δ	P_r
1.2171	1	4	$162 \frac{rad}{s}$	$4 \frac{rad}{s}$	$4.8.\ 10^6$ W

Table 3-6: Sensors model parameters.

m_w	σ_w	$m_{\omega r}$	$\sigma_{\omega r}$	$m_{\omega g}$	$\sigma_{\omega g}$
$1.5 \frac{m}{s}$	$0.5 \frac{m}{s}$	$0 \frac{rad}{s}$	$0.025 \frac{rad}{s}$	$0 \frac{rad}{s}$	$0.05 \frac{rad}{s}$
$m_{\tau g}$	$\sigma_{\tau g}$	m_{Pg}	σ_{Pg}	m_β	σ_β
0 Nm	90 Nm	0 W	$1.\ 10^3$ W	0^o	0.2^o

3.4.2 Faults Description

Table 3-7 illustrate the faults to be applied on the benchmark model. This table classifies the faults regarding their locations, class, type, value, and time of development. Each fault will be applied alone on the benchmark model to study the effects of each fault on the performance on wind turbine.

Table 3-7: The faults scenario applied on the benchmark model.

Fault Location	Fault #	Fault Class	Fault Type & Value		Fault Time & Duration
Generator Speed Measurement	F1	Sensor Faults	constant $\omega_{g,m}$ step	-20 rad/sec	2000-3500 s
Rotor Speed Measurement	F2		constant $\omega_{r,m}$ step	-0.32 rad/sec	
Pitch Position Measurement	F3		constant $\beta_{1,m}$	5^o	
	F4		constant $\beta_{2,m}$	10^o	
	F5		constant $\beta_{3,m}$	15^o	

Chapter Four

Simulation Results

This chapter shows the corresponding effects of the different sensor faults on the performance of wind turbine by applying these faults separately on the wind turbine benchmark model.

4.1 Wind speed profile

Figure 4.1 shows wind speed profile applied on the benchmark model. This profile consists of real wind speed data that was collected and tested on this model.

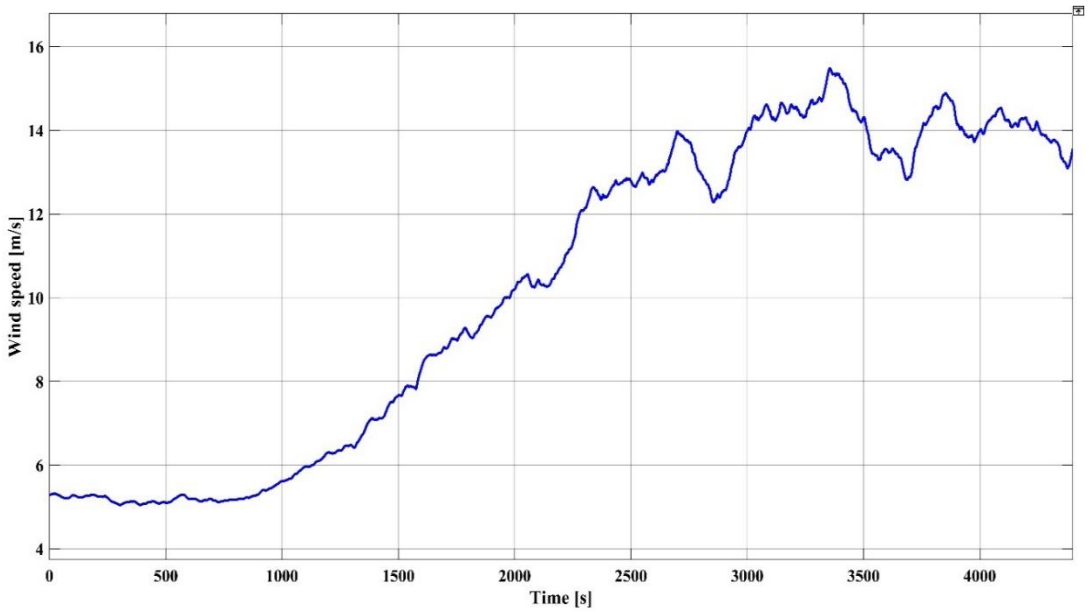

Figure 4.1: wind speed profile applied on the benchmark model.

4.2 Controller Behavior

Figure 4.2 shows switching behavior of the controller between the two control modes. Value of "0" represents "control mode 1" which is power optimization mode. The power is optimized in this mode as long as wind speed is less than 12.5 m/s. The other control mode (which is illustrated by the value of "1") is "control mode 2" which represents power reference following mode. In this mode, the power is maintained at the rated value when wind speed is between 12.5 – 25 m/s. it is worth mentioned that this controller behavior is at the healthy operation (without applying any faults). When faults exist, this behavior may change.

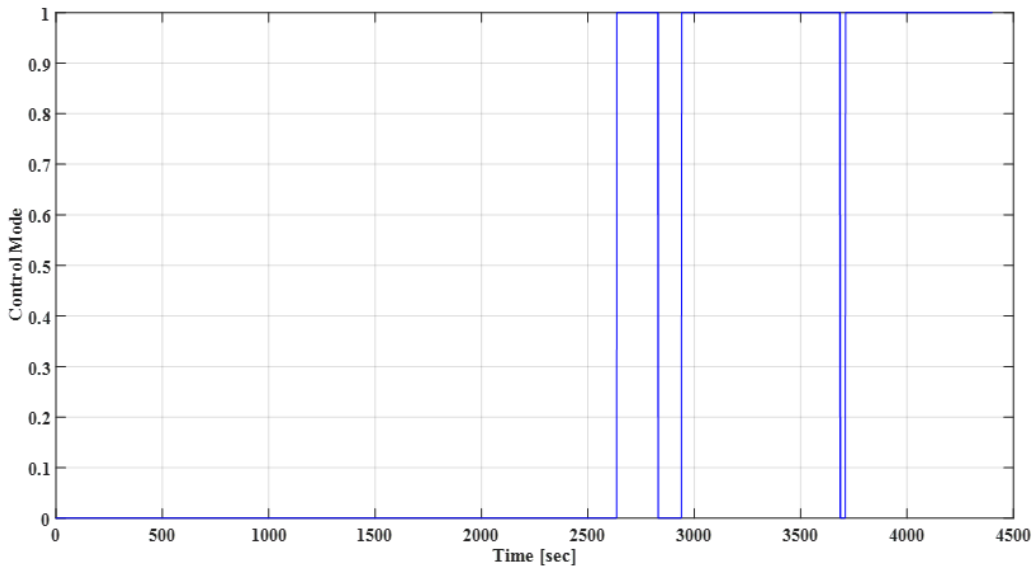

Figure 4.2: Controller switching behavior between the two control modes.

4.3 Generator Speed Sensor Fault

Fault 1 represents a constant step fault in the generator speed measurement, i.e. the value of measured ω_g is not correct. Figure 4.3 shows ω_g measurement during the whole simulation time without and with applying fault 1. Faulty step value of ω_g measurement -20 rad/sec during the unified faults time (2000 – 3500 s).

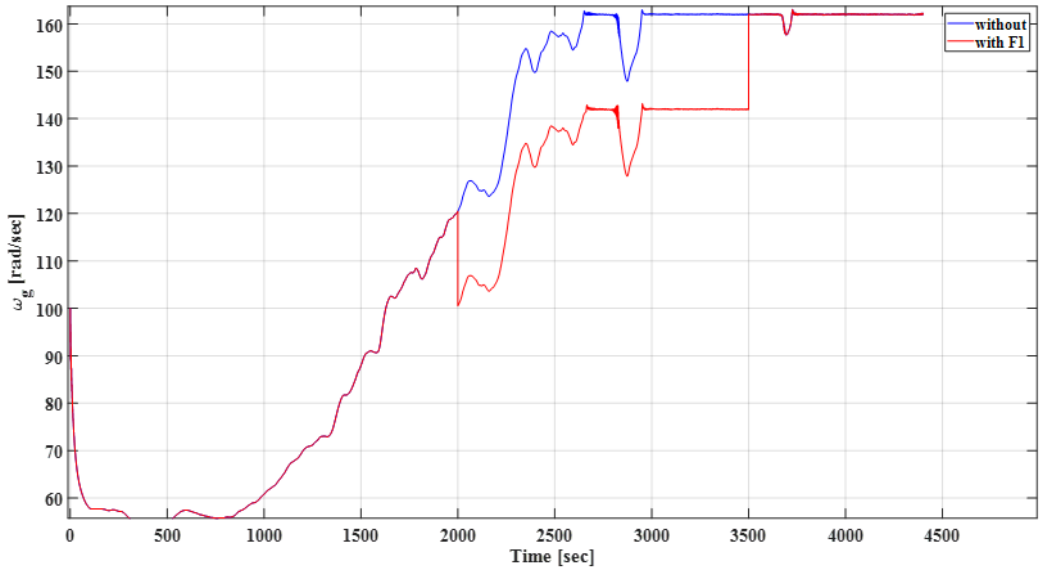

Figure 4.3: ω_g measurement without and with applying fault 1.

Figure 4.4 shows switching behavior of the controller between the two control modes during fault occurrence. Controller behavior has no changes compared to the healthy behavior.

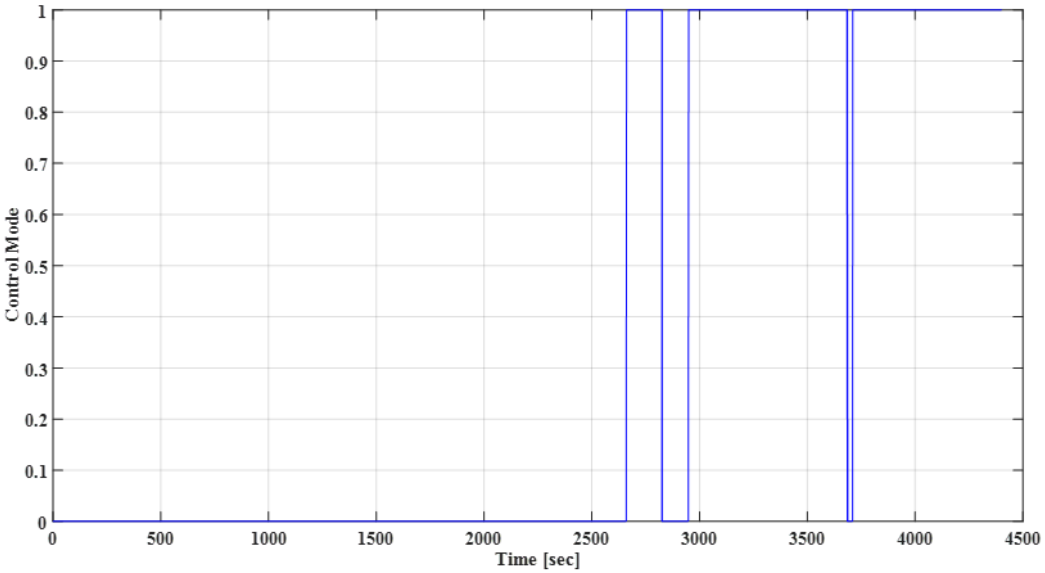

Figure 4.4: Controller switching behavior between the two control modes during fault 1.

Figure 4.5 shows the values of generated power (P_g) without and with applying fault 1. It is obvious that it is decreased as ω_g decreased, generated power reduction is about 12%. The effects of this fault on the generated power are logical and justified since the generator speed is reduced by about 14%.

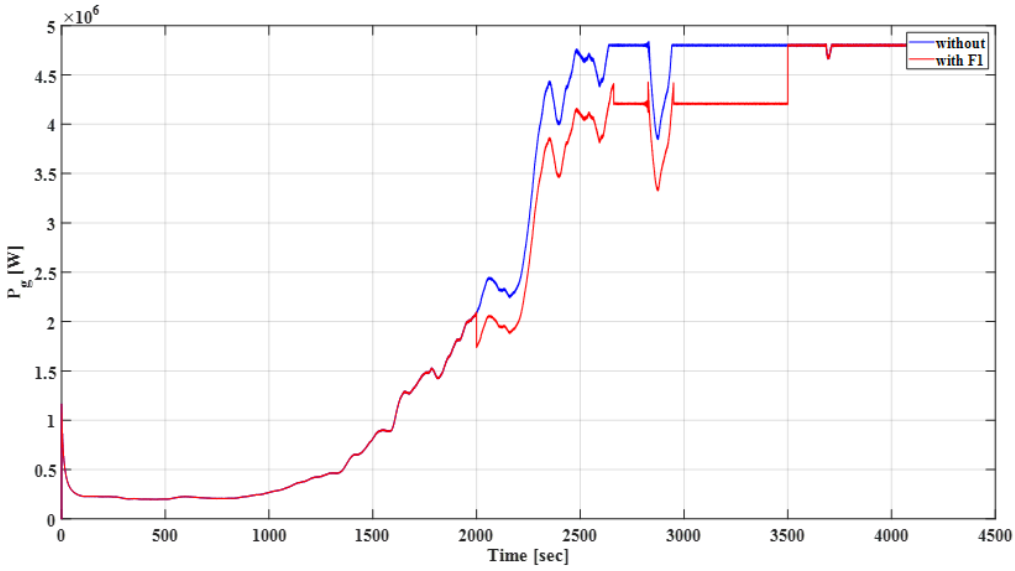

Figure 4.5: P_g measurement without and with applying fault 1.

4.4 Rotor Speed Sensor Fault

Fault 2 represents a constant step fault in the rotor speed measurement, i.e. the value of measured ω_r is not correct. Figure 4.6 shows ω_r measurement (shaft speed measurements) during the whole simulation time without and with applying fault 2. The faulty step value is about -0.3 rad/s which represents about 18% of the steady state healthy value. The time duration of all faults is unified (between 2000 – 3500 s).

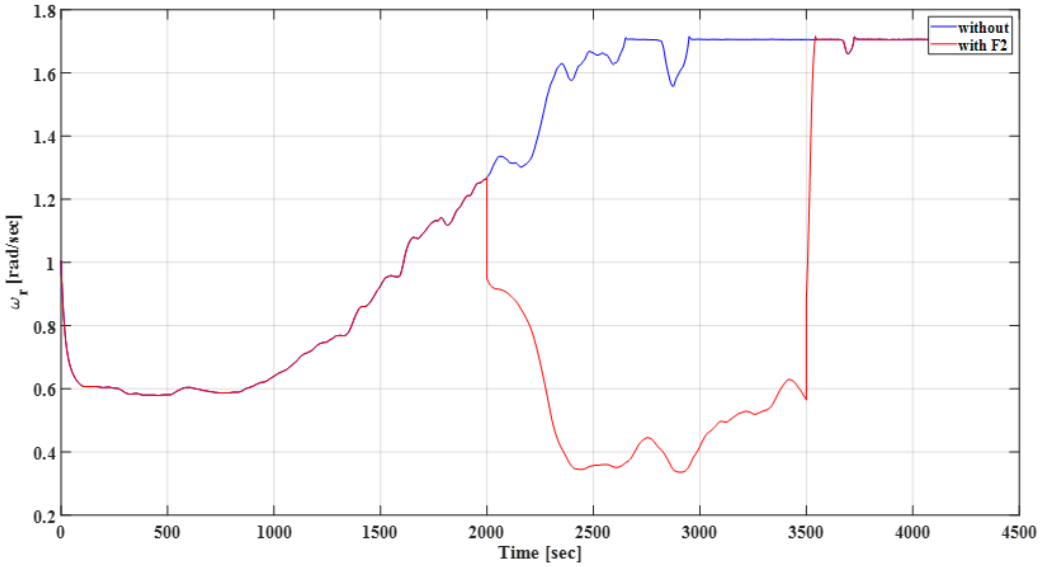

Figure 4.6: ω_r measurement without and with applying fault 2.

Figure 4.7 shows switching behavior of the controller between the two control modes during fault occurrence. Controller stay at mode 1 (without any switching) during the whole fault duration.

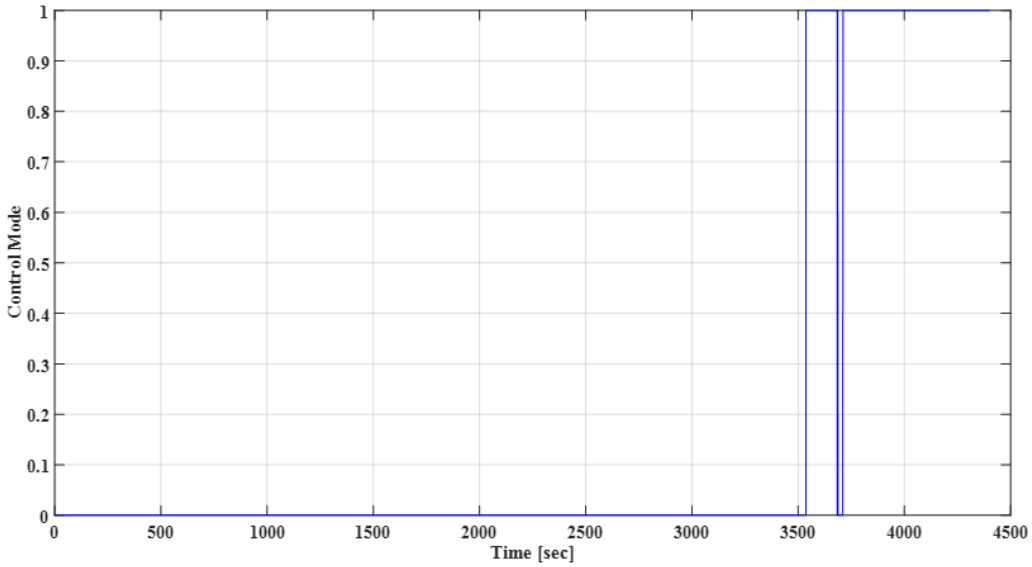

Figure 4.7: Controller switching behavior between the two control modes during fault 2.

Rotor torque is strongly affected by the faulty rotor speed. Figure 4.8 shows that rotor torque magnitude is decreased to 27% of its magnitude at the healthy situation.

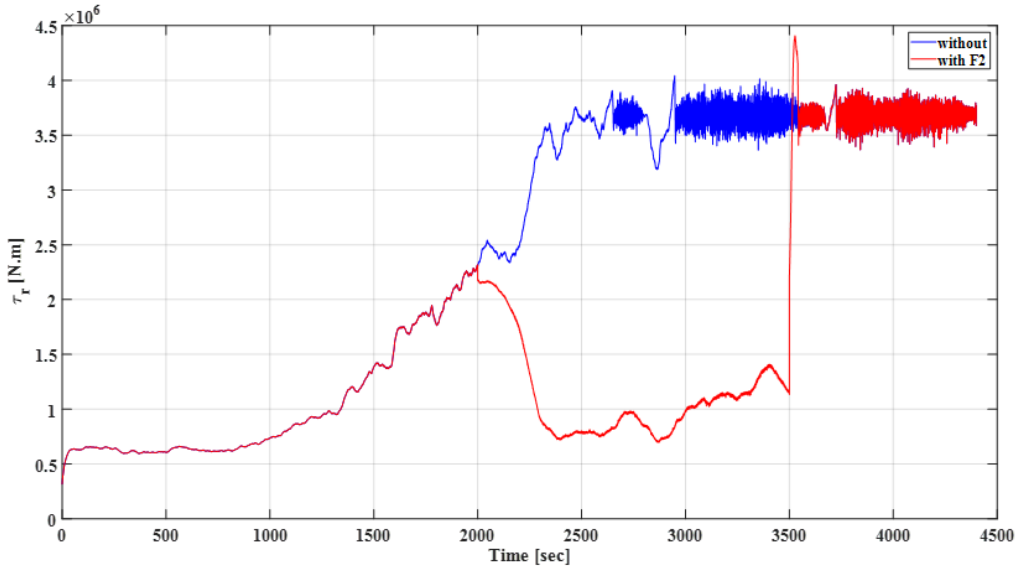

Figure 4.8: τ_r measurement without and with applying fault 2.

Figure 4.9 shows generator speed profile of the wind turbine model. It is noticed that the reduction percentage is the same as in rotor torque. The reduction behavior is severe and follows the occurred reduction of rotor speed.

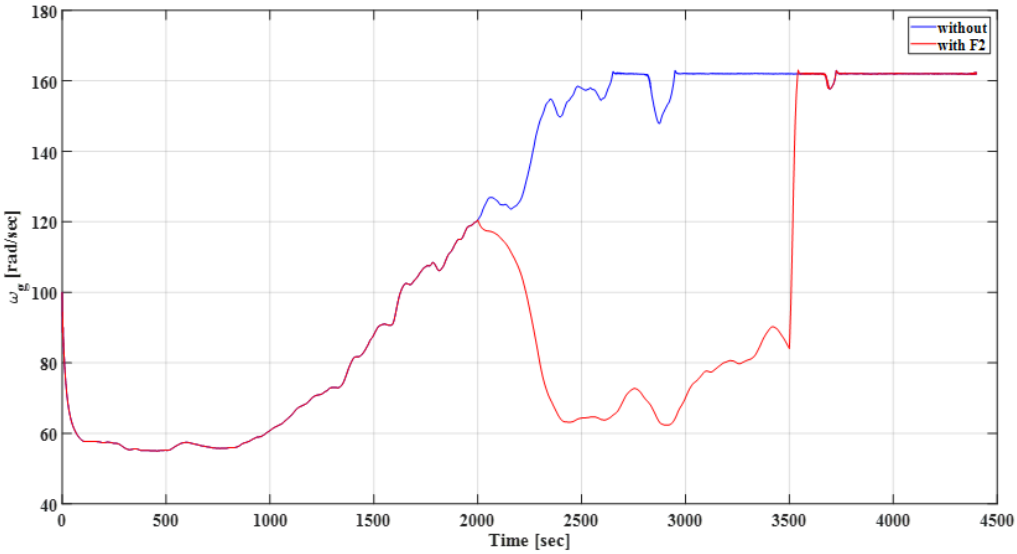

Figure 4.9: ω_g measurement without and with applying fault 2.

Generated torque is also strongly affected. It decreased by 83% compared to its steady state healthy value as shown in Figure 4.10. It is noticed that generated torque available during fault existence is 17% whereas rotor torque available value was 27% during fault existence.

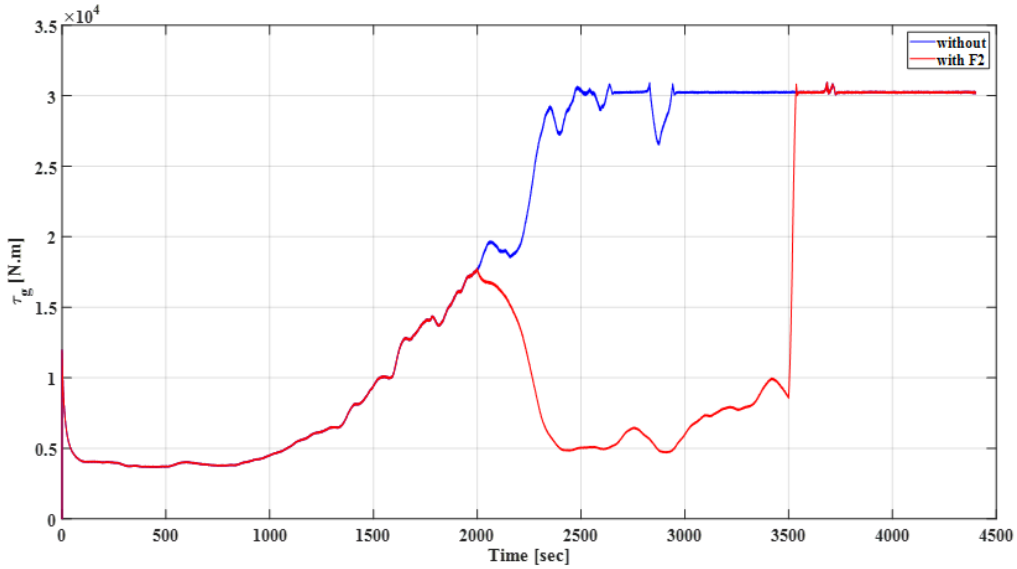

Figure 4.10: τ_g measurement without and with applying fault 2.

Reduction in both rotor speed and rotor torque will have a strong negative impact on the generated power which is the output of the whole wind turbine. This is clearly seen in Figure 4.11. Generated power is decreased from 4.8 MW (rated power) to about 0.5 MW due to fault existence, i.e., just 10% of the generated power is available during fault time.

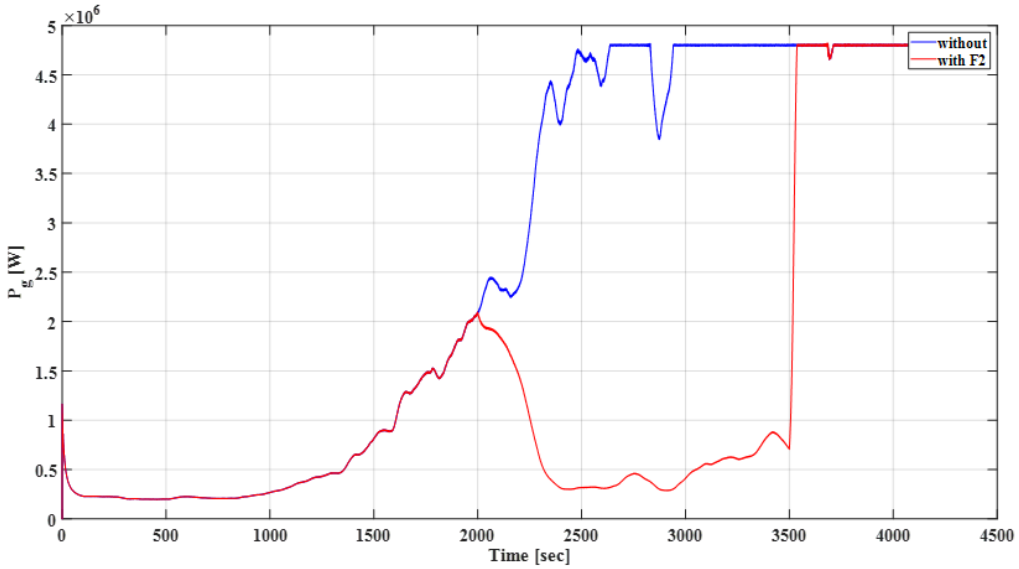

Figure 4.11: P_g measurement without and with applying fault 2.

4.5 Pitch Position Sensor Fault (1st Blade)

Fault 3 is applied on the first pitch angle (β_1) with a constant fault value (5°) during the unified fault duration (2000 – 3500 s). Figure 4.12 shows switching behavior of the controller between the two control modes during fault occurrence. Controller behavior has no changes compared to the healthy behavior.

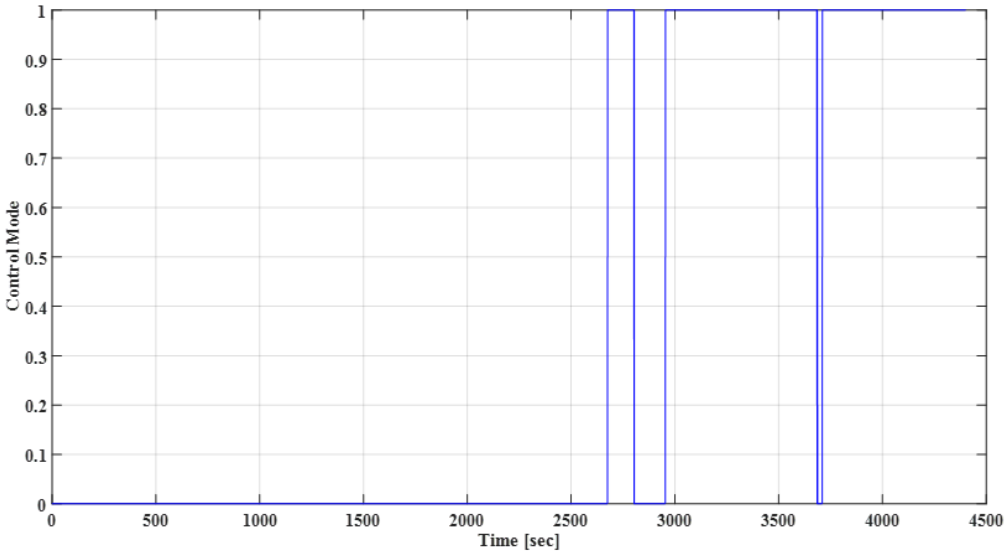

Figure 4.12: Controller switching behavior between the two control modes during fault 3.

Figure 4.13 shows a little effect of this fault on rotor speed. This effect represents about 5% reduction (in average) during fault duration period.

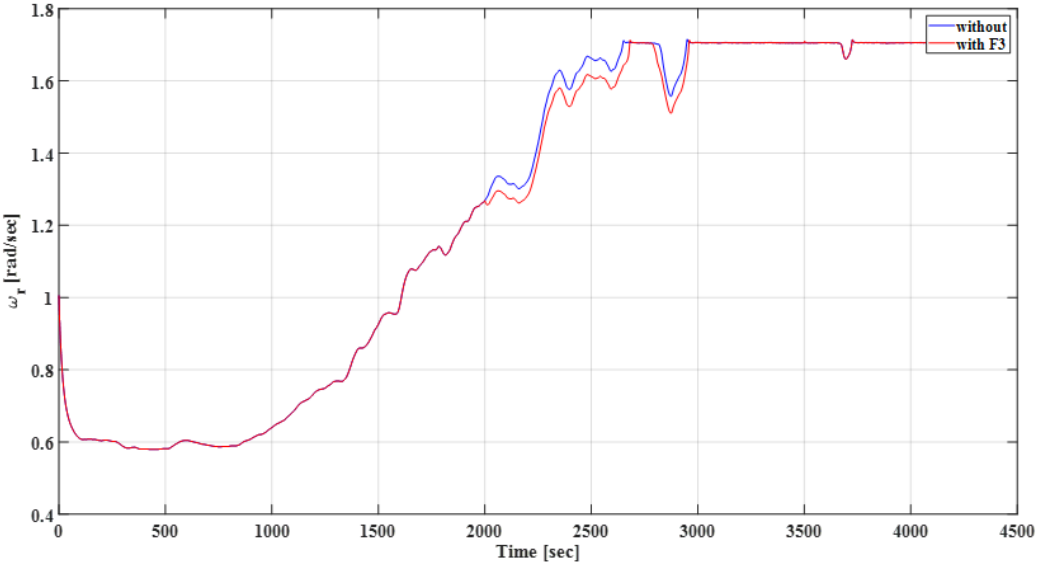

Figure 4.13: ω_r measurement without and with applying fault 3.

Rotor torque is also slightly affected with the same reduction behavior of rotor speed as shown in Figure 4.14.

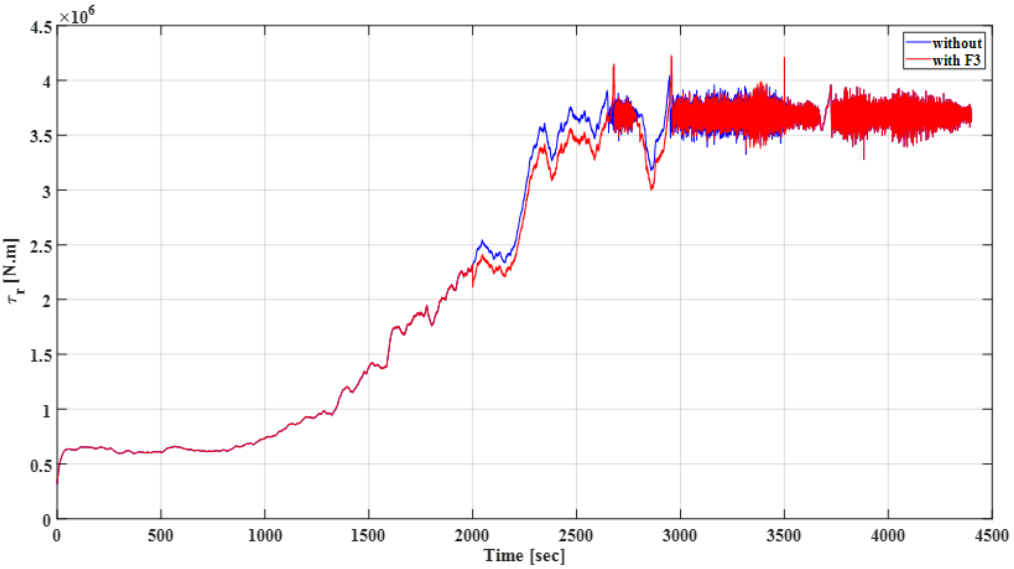

Figure 4.14: τ_r measurement without and with applying fault 3.

Figures 4.15 and 4.16 show that generator speed and generator torque behaviors are typically same as rotor speed behavior during fault duration time. Fault occurrence cause a

reduction of about 4% in generator speed whereas generator torque is reduced by about 6% (in average).

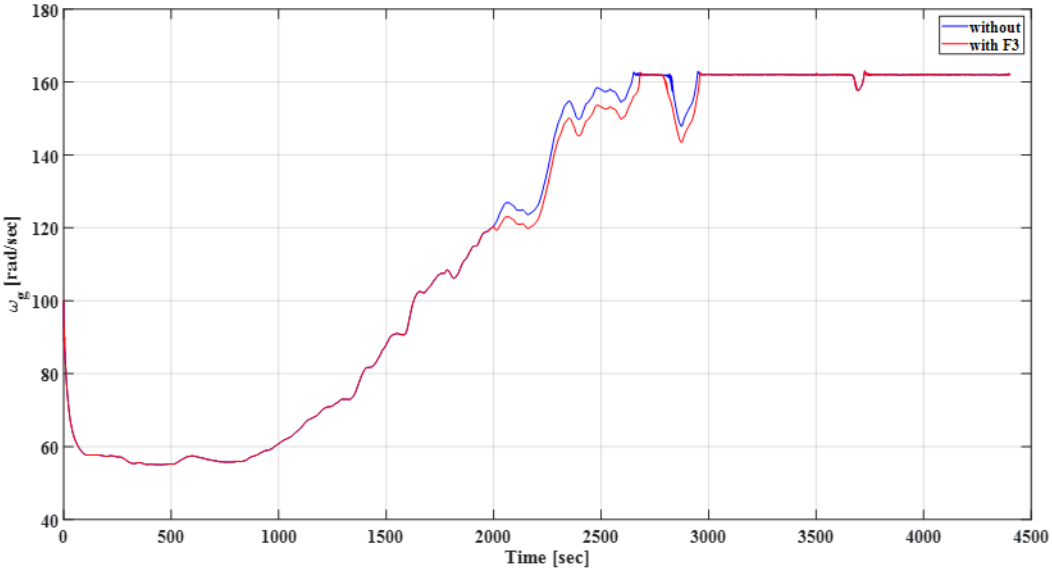

Figure 4.15: ω_g measurement without and with applying fault 3.

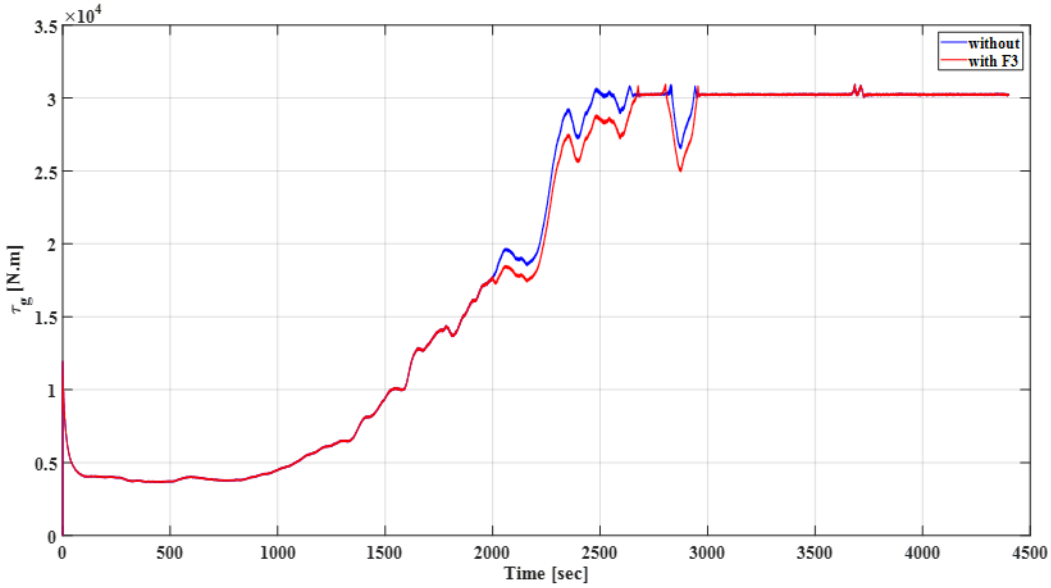

Figure 4.16: τ_g measurement without and with applying fault 3.

Consequently, generated power is negatively affected during the fault duration time. Generated power reduction reaches to 10% at the middle of fault duration time as shown in Figure 4.17. Generated power behaves same as rotor speed, generator speed, and generator torque during fault occurrence.

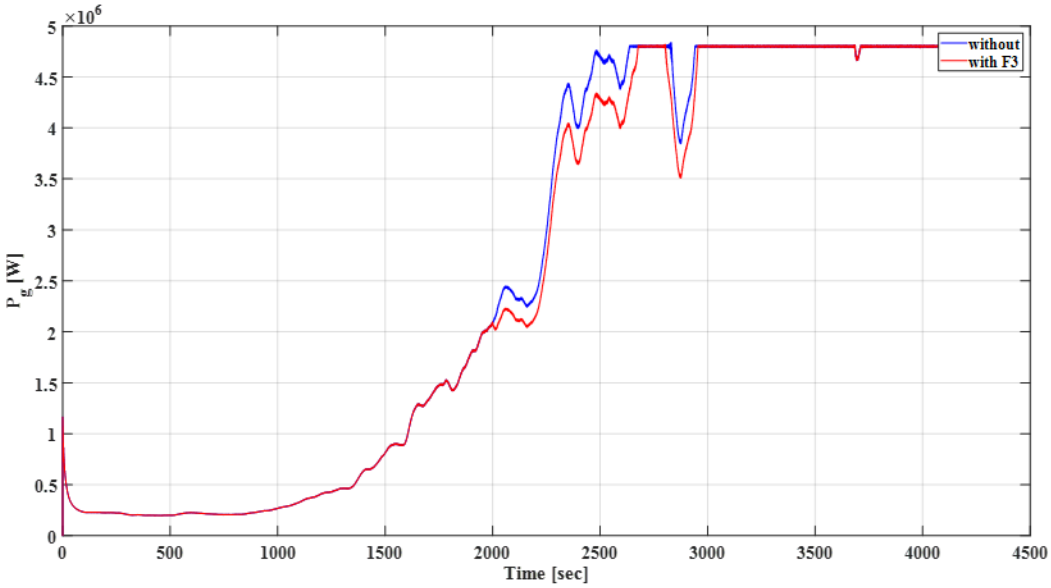

Figure 4.17: P_g measurement without and with applying fault 3.

4.6 Pitch Position Sensor Fault (2nd Blade)

Fault 4 is applied on the second pitch angle (β_2) with a constant fault value (10^o) during the unified fault duration (2000 – 3500 s). Figure 4.18 shows switching behavior of the controller between the two control modes during fault occurrence. Controller behavior shows one switching action between the two control modes compared with 3 switching times during the healthy behavior.

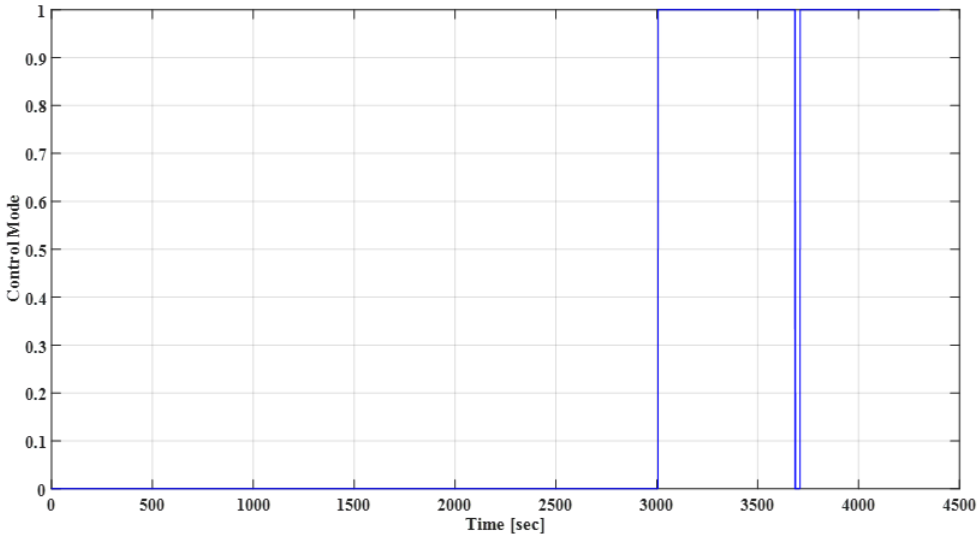

Figure 4.18: Controller switching behavior between the two control modes during fault 4.

Figure 4.19 shows a significant effect of this fault on rotor speed. This effect represents about 8% reduction (in average) during fault duration period.

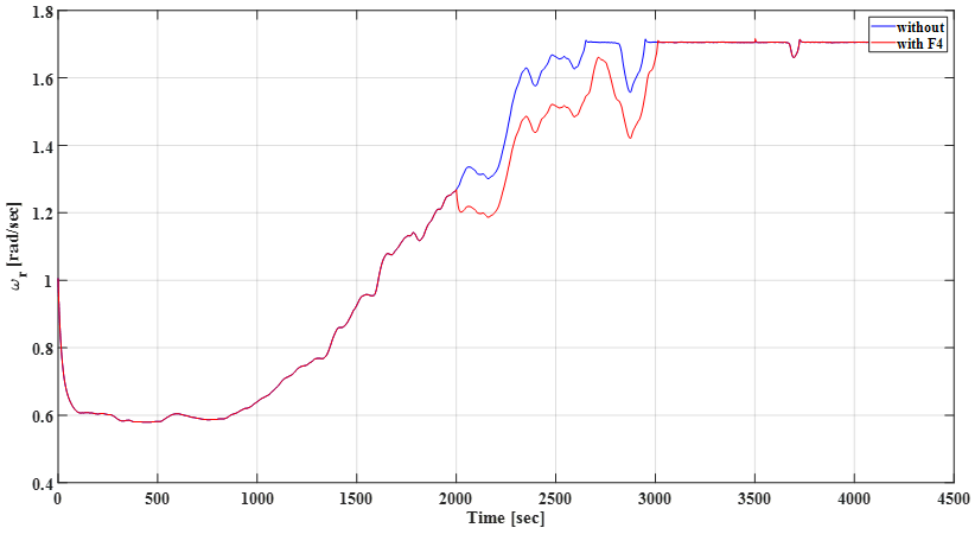

Figure 4.19: ω_r measurement without and with applying fault 4.

Rotor torque is also s affected significantly by fault 4. Rotor torque reduction reaches to 16% at sometimes during fault occurrence time as shown in Figure 4.20.

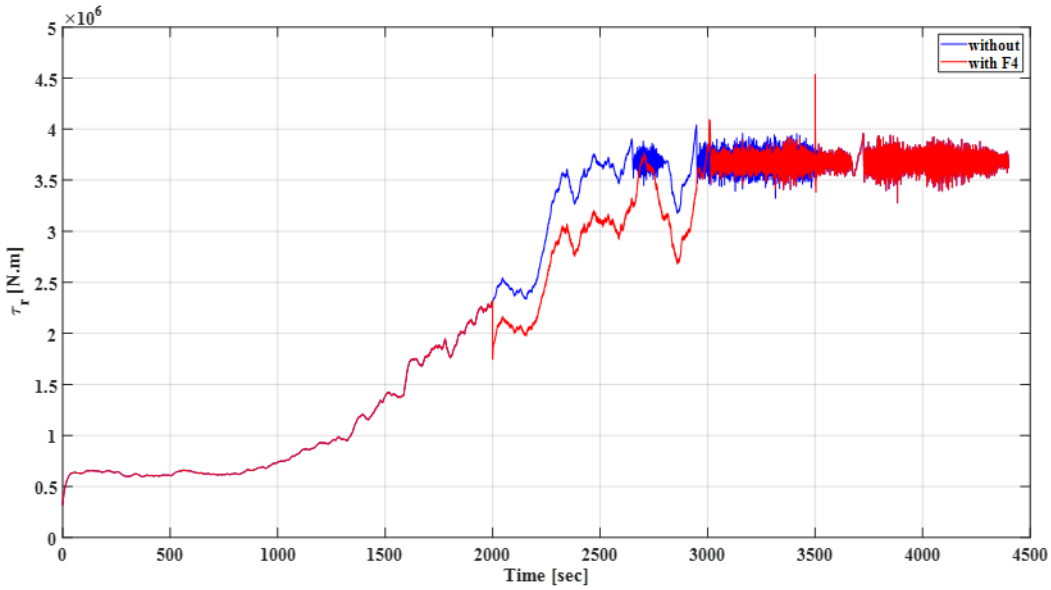

Figure 4.20: τ_r measurement without and with applying fault 4.

Figures 4.21 and 4.22 show that generator speed and generator torque behaviors are typically same as rotor speed behavior during fault duration time. Fault occurrence cause a

reduction of about 10% in generator speed whereas generator torque is reduced by about 18% (in average).

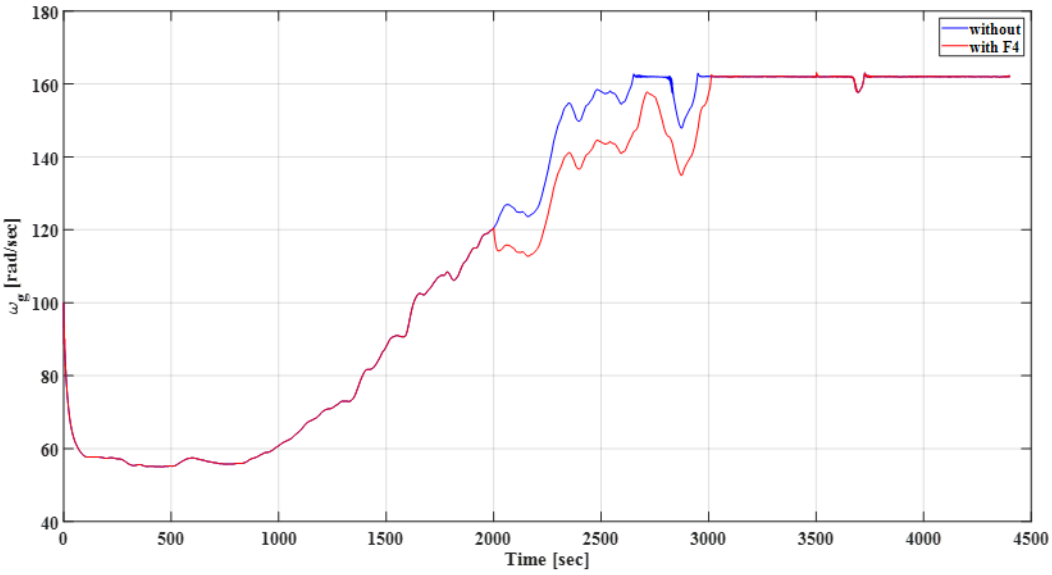

Figure 4.21: ω_g measurement without and with applying fault 4.

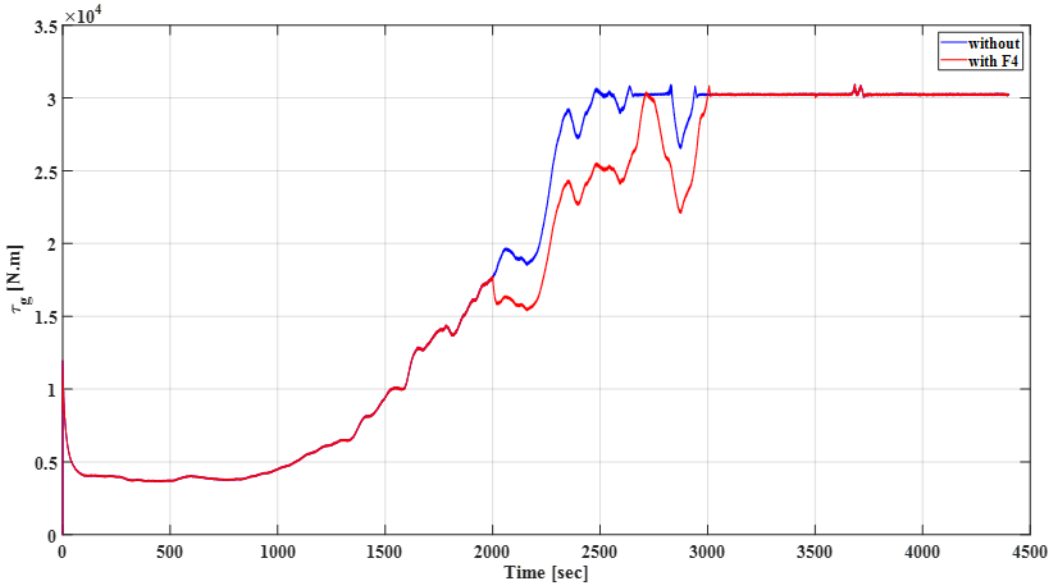

Figure 4.22: τ_g measurement without and with applying fault 4.

Generated power is also affected during the fault duration time. Generated power reduction reaches to 25% at some fault duration times as shown in Figure 4.23. Generated power behaves same as rotor speed, generator speed, and generator torque during fault occurrence.

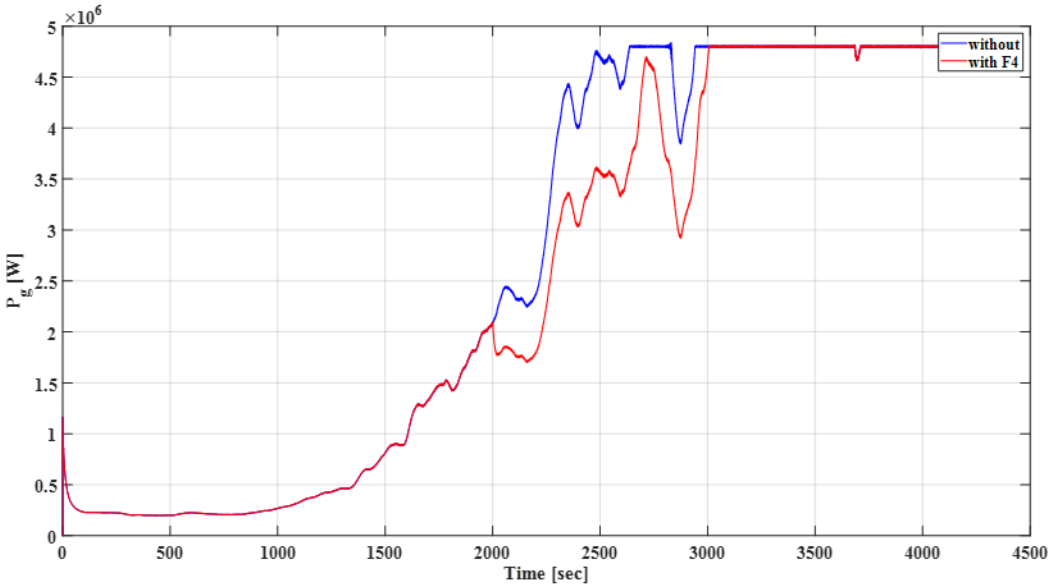

Figure 4.23: P_g measurement without and with applying fault 4.

4.7 Pitch Position Sensor Fault (3rd Blade)

Fault 5 is applied on the third pitch angle (β_3) with a higher constant fault value (15°) during the unified fault duration (2000 – 3500 s). Figure 4.24 shows switching behavior of the controller between the two control modes during fault occurrence. Controller behavior also shows 3 switching actions between the two control modes but at different times compared to the controller healthy behavior.

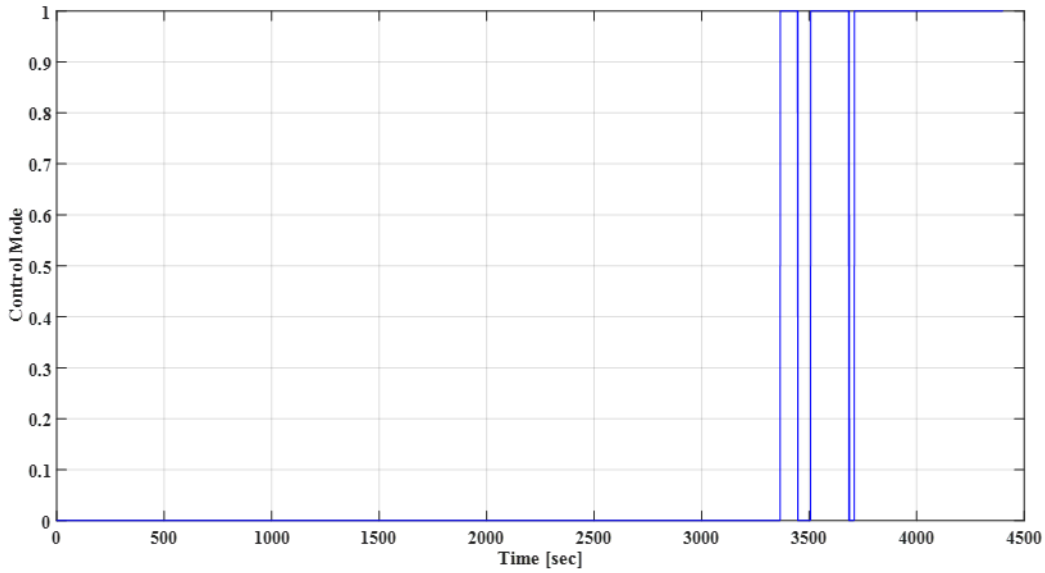

Figure 4.24: Controller switching behavior between the two control modes during fault 5.

Figure 4.25 shows more significant effect of this fault on rotor speed. This effect represents about 15% reduction (in average) during fault duration period.

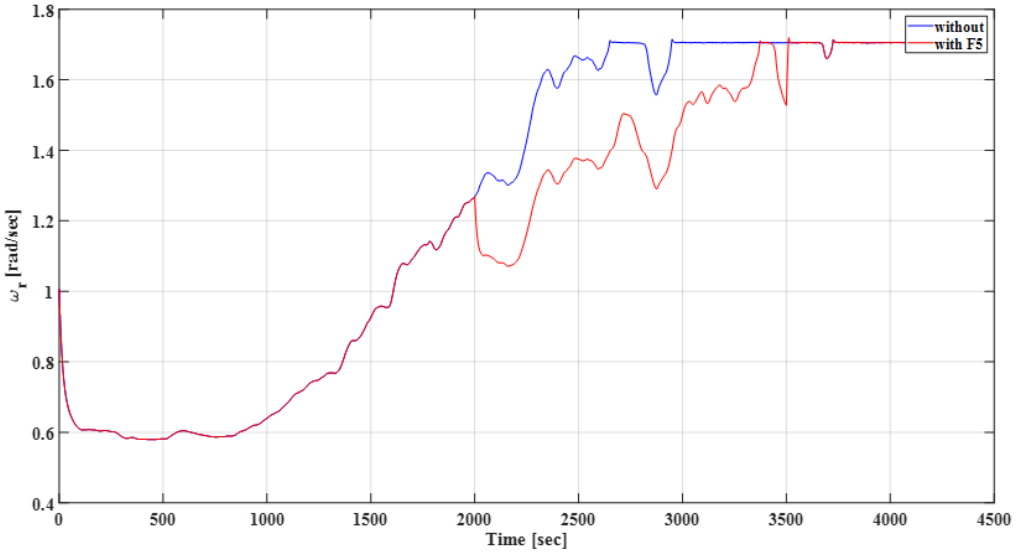

Figure 4.25: ω_r measurement without and with applying fault 5.

Rotor torque is also affected significantly but in a non-uniform manner when the fault starts and ends as shown in Figure 4.26. Rotor torque drops sharply when the fault starts and increases sharply when the fault ends. Other than the fault period limits, rotor torque dropped in a predicted manner as previous reduction behaviors. Rotor torque reduction reaches to 28% at the middle of fault occurrence time.

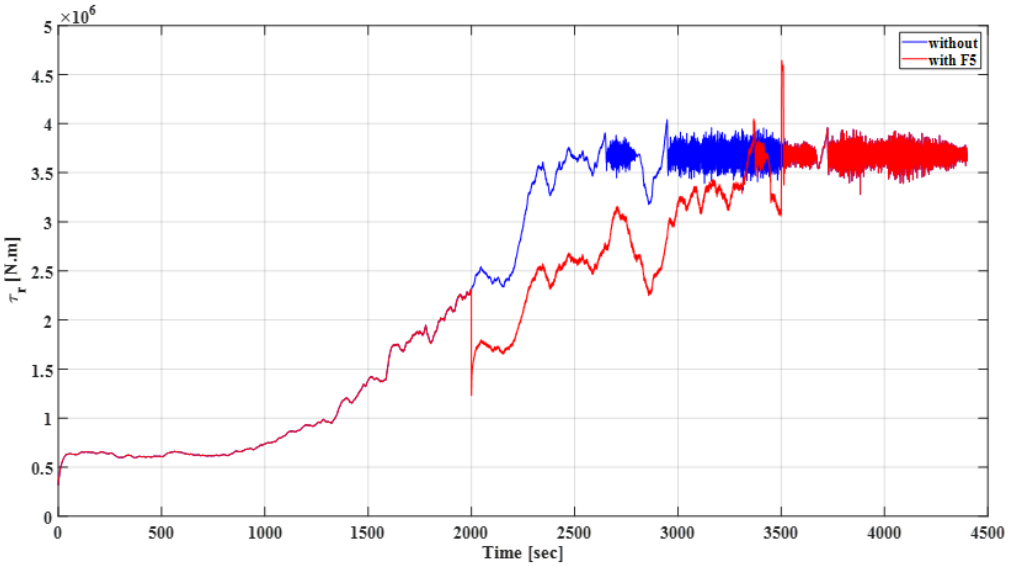

Figure 4.26: τ_r measurement without and with applying fault 5.

Figures 4.27 and 4.28 show that generator speed and generator torque behaviors are typically same as rotor speed behavior during fault time. Fault occurrence cause a reduction

of about 13% in generator speed whereas generator torque is reduced by about 25% (in average).

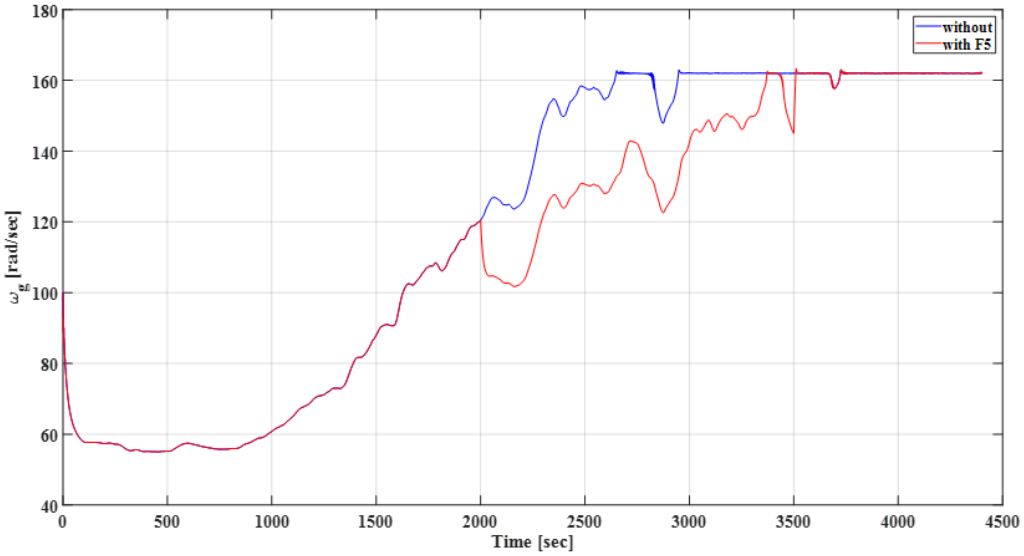

Figure 4.27: ω_g measurement without and with applying fault 5.

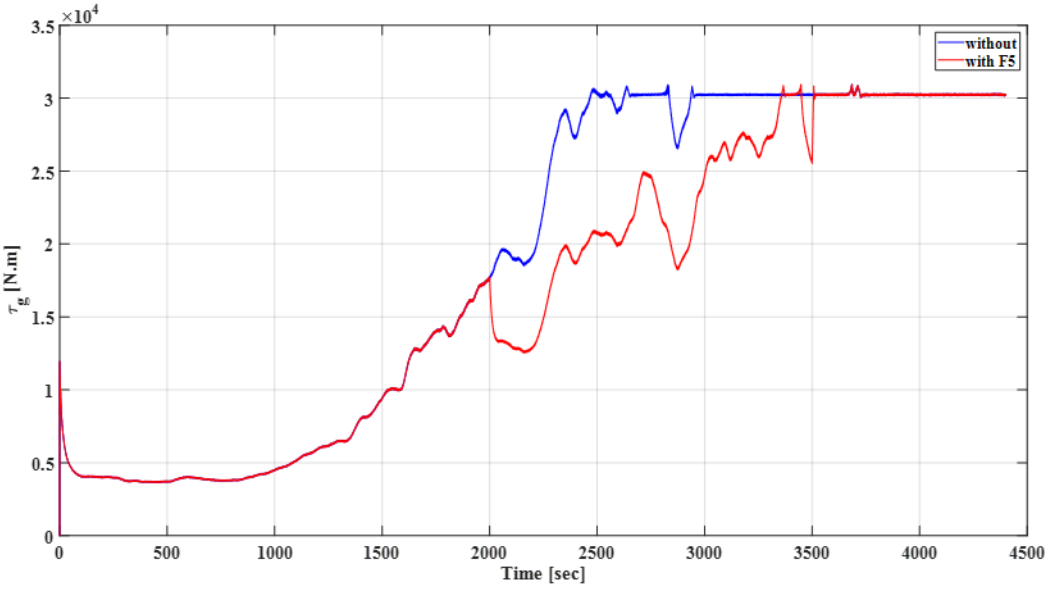

Figure 4.28: τ_g measurement without and with applying fault 5.

Consequently, generated power is highly affected during the fault time. Generated power dropped from 4.7 MW to 2.6 MW at sometimes during the fault occurrence, i.e., 45% reduction in power generated as shown in Figure 4.29. In average, power generated is decreased by 35% during fault occurrence time. Power generated behaves same as rotor speed, generator speed, and generator torque during fault occurrence.

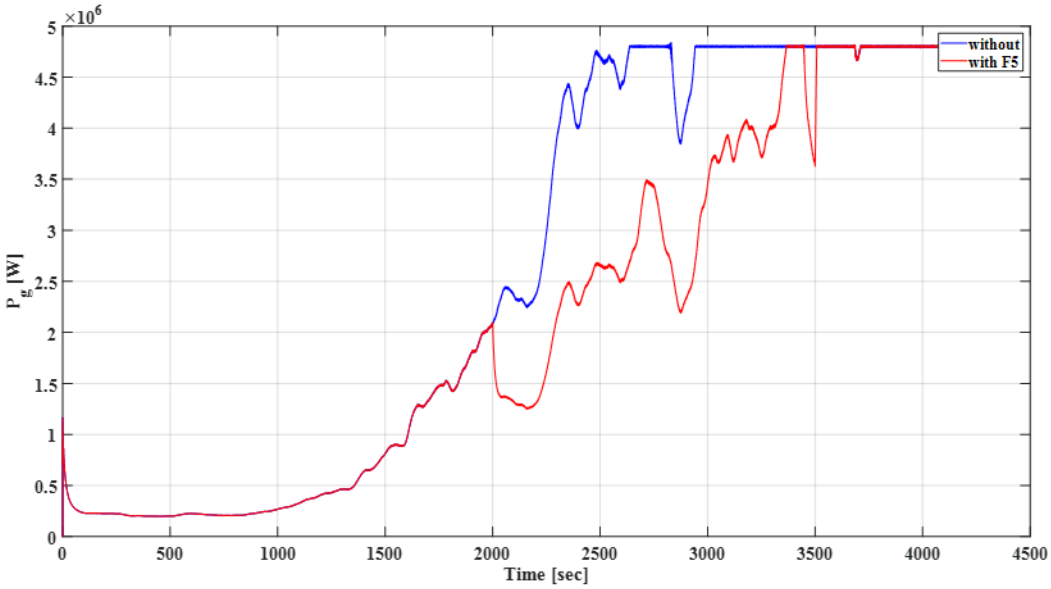

Figure 4.29: P_g measurement without and with applying fault 5.

4.8 Concluding Remarks

It is obvious from the results above that the sensors' faults harm the performance of the wind turbine. Therefore, integration of fault diagnosis and fault-tolerant control in the wind turbine systems will play an important role to improve the output of the turbine and also in on-time monitoring of the turbine behavior. The developed scheme should overcome the sensor faults and replaced the sensor's faulty measurements with the correct ones under the constraint that the fault-tolerant control scheme will not affect the safe operation of the turbine.

Chapter Five

Detection Filter and FTC Algorithm

This chapter will deal with the sensors faults detectability process and the proposed FTC algorithm in order to reconstruct the missing measurements signals.

5.1 Detection Filter Formulation

Recall the state space representation of a linear time-invariant system:

$$\dot{\boldsymbol{x}} = \boldsymbol{Ax} + \boldsymbol{Bu} \tag{5.1a}$$

$$\boldsymbol{y} = \boldsymbol{Cx} + \boldsymbol{Du} \tag{5.1b}$$

Where:

- x = state vector = $[\omega_g, \omega_r, \beta_1, \beta_2, \beta_3]^T$
- u = input vector
- y = output vector
- A = system matrix
- B = input matrix
- C = output matrix
- D = feedthrough matrix

Consider a full order observer of the form [87]:

$$\hat{\boldsymbol{x}} = \boldsymbol{A}\hat{\boldsymbol{x}} + \boldsymbol{Bu} - \boldsymbol{L}(\boldsymbol{y} - \hat{\boldsymbol{y}}) \tag{5.2a}$$

$$\hat{\boldsymbol{y}} = \boldsymbol{C}\hat{\boldsymbol{x}} + \boldsymbol{Du} \tag{5.2b}$$

Where:

- $\hat{\boldsymbol{x}} =$ state estimation
- $\hat{\boldsymbol{y}} =$ output estimation
- $\boldsymbol{L} =$ observer matrix

The state estimation error: $\boldsymbol{e} = \boldsymbol{x} - \hat{\boldsymbol{x}}$

The state estimation error: $\dot{\boldsymbol{e}} = \dot{\boldsymbol{x}} - \hat{\dot{\boldsymbol{x}}}$

The residual: $\boldsymbol{r} = \boldsymbol{y} - \hat{\boldsymbol{y}}$

When there is no disturbances or modelling errors, residual will be nonzero only if there are one or more faults in the system, i.e., the fault/s is/are detected by the detection filter (a full-order observer). It follows that the stable observer can detect the fault/s by only monitoring the residual, and when this residual deviates from zero, a fault has occurred.

5.2 Residual Evaluation and Threshold Setting

After detection filter have been formulated, evaluation of the resulting residual signal become the next step. The threshold setting should be also defined in order to achieve an accurate detection process. Different techniques could be used for evaluation and defining threshold setting. In this thesis, RMS technique with a moving window is used for residual signals evaluation.

A. Residual Evaluation

RMS value of the residual signal $\boldsymbol{r}$, for the discrete time case, is defined by [88]:

$$J_{RMS} = \|r(k)\|_{RMS} = \left(\frac{1}{N} \sum_{j=1}^{N} \|r(k+j)\|^2 \right)^{1/2} \tag{5.3}$$

J_{RMS} measure the average energy of the residual signal $\boldsymbol{r}$ over the interval (k, k+N).

B. Threshold setting

threshold determination is to evaluate the tolerance limit for system disturbances (mainly sensors disturbance) during the healthy (fault-free) operation. In this thesis, the threshold is considered as the maximum effect of system disturbances on the residual signal in the healthy (fault-free) operation.

Suppose that $\boldsymbol{d_r}$ is bounded by and in the sense of:

$$\|d_r\|_{RMS} \leq \delta_d \tag{5.4}$$

where $\boldsymbol{\delta_d}$ is bounded of system disturbances (mainly sensors disturbances).

Then the threshold $\boldsymbol{J_{th,RMS}}$ is defined by:

$$J_{th,RMS} = \sup_{\substack{\|d_r\|_{RMS} \leq \delta_d \\ f = 0}} J_{RMS} \tag{5.5}$$

The detection logic then becomes:

$\boldsymbol{J_{RMS} > J_{th,RMS}}$ ➔ Alarm, a fault is detected

$\boldsymbol{J_{RMS} \leq J_{th,RMS}}$ ➔ No alarm, fault-free

C. Simulation Results

This subsection shows numerical simulation values of state space matrices, observer parameters, the numerical threshold value (in fault-free conditions), and numerical residual values for all state variables [ω_g, ω_r, β_1, β_2, β_3].

1. State space and observer matrix parameter

- **Blade and pitch subsystem:**

  The state-space representation of the blade and pitch subsystem is driven from Eq. (3.5), the numerical values of this subsystem are as follows:

$$A_{pb} = \begin{bmatrix} -13.3320 & -123.4321 \\ 1.00 & 0 \end{bmatrix}$$

$$B_{pb} = \begin{bmatrix} 1 \\ 0 \end{bmatrix}$$

$$C_{pb} = [0 \quad 123.4321]$$

$$D_{pb} = 0$$

$$Eigen\ Values = [-3 \quad -4]$$

$$L_{pb} = \begin{bmatrix} -0.2189 \\ -0.0513 \end{bmatrix}$$

- **Drive train subsystem:**
- The state-space representation of the drive train subsystem is driven from Eqs. (3.7)-(3.9), the numerical values of this subsystem are as follows:

$$A_{ddt} = 10000 * \begin{bmatrix} -0 & 0 & -0.0049 \\ 0 & -0 & 7.0688 \\ 0.0001 & -0 & 0 \end{bmatrix}$$

$$B_{ddt} = \begin{bmatrix} 0 & 0 \\ 0 & -0.0026 \\ 0 & 0 \end{bmatrix}$$

$$C_{ddt} = \begin{bmatrix} 1 & 0 & 0 \\ 0 & 1 & 0 \end{bmatrix}$$

$$D_{ddt} = \begin{bmatrix} 0 & 0 \\ 0 & 0 \end{bmatrix}$$

$$Eigen\,Values = [-0.1 \quad -0.2 \quad -0.3]$$

$$L_{ddt} = \begin{bmatrix} -0.0643 & -0.0003 \\ 524.6209 & 0.5472 \\ 1.0011 & -0.0105 \end{bmatrix}$$

It is important to mention here that the linearized subsystems of the wind turbine are of 2nd and 3rd order which enable it to be suitable for online implementation.

Figure 5.1 shows the numerical threshold value during fault-free operation which is equal 1.6, this value expressed system disturbances (mainly sensors disturbance).

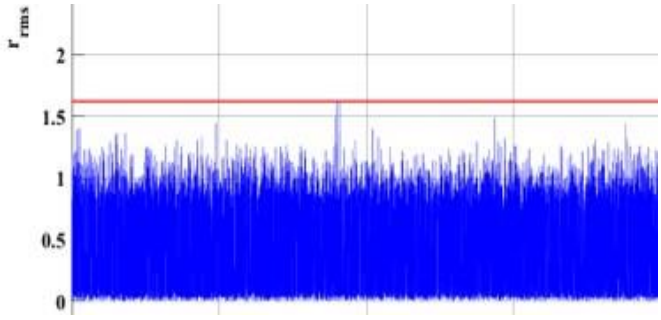

Figure 5.1: the threshold value during fault-free operation.

Figure 5.2 show the residual value during fault 1 occurrence (when ω_g is faulty). The residual value is more than 100 times of threshold value, i.e., easy and direct fault detection.

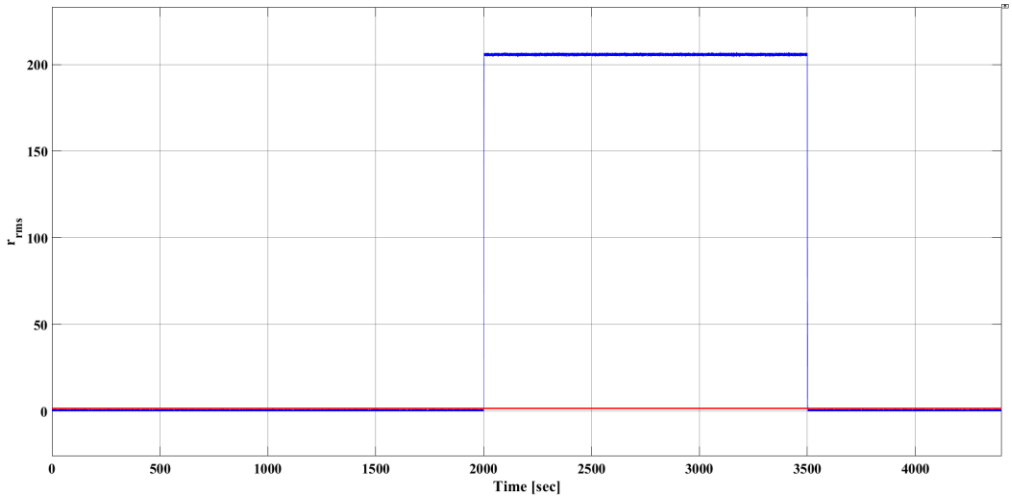

Figure 5.2: Residual value during fault 1 occurrence (when ω_g is faulty).

Figure 5.3 show the residual value during fault 2 occurrence (when ω_r is faulty). The residual value is completely above the threshold value, i.e., the fault will be easily detected.

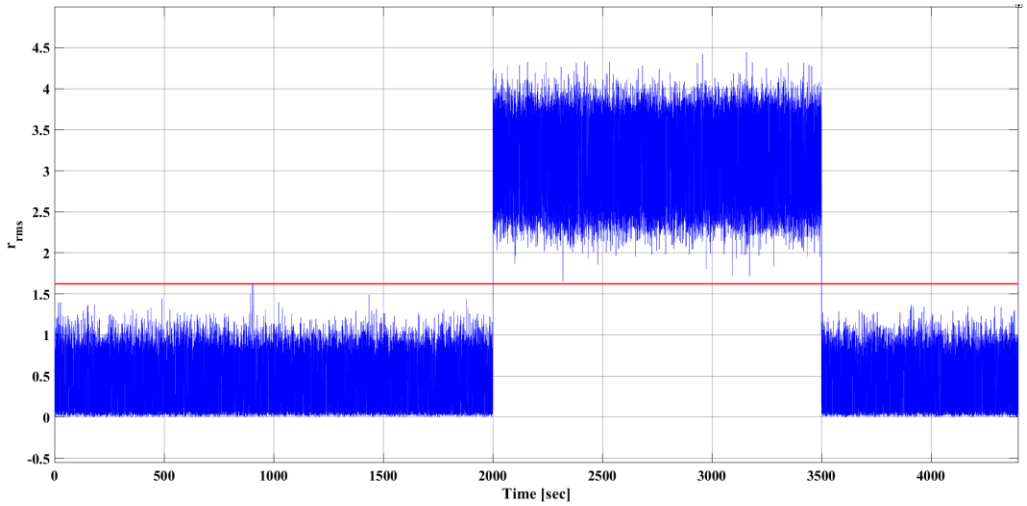

Figure 5.3: Residual value during fault 2 occurrence (when ω_r is faulty).

Figure 5.4 show the residual value during fault 3 occurrence (when β_1 is faulty). The residual value is more than 30 times of threshold value, i.e., easy and direct fault detection.

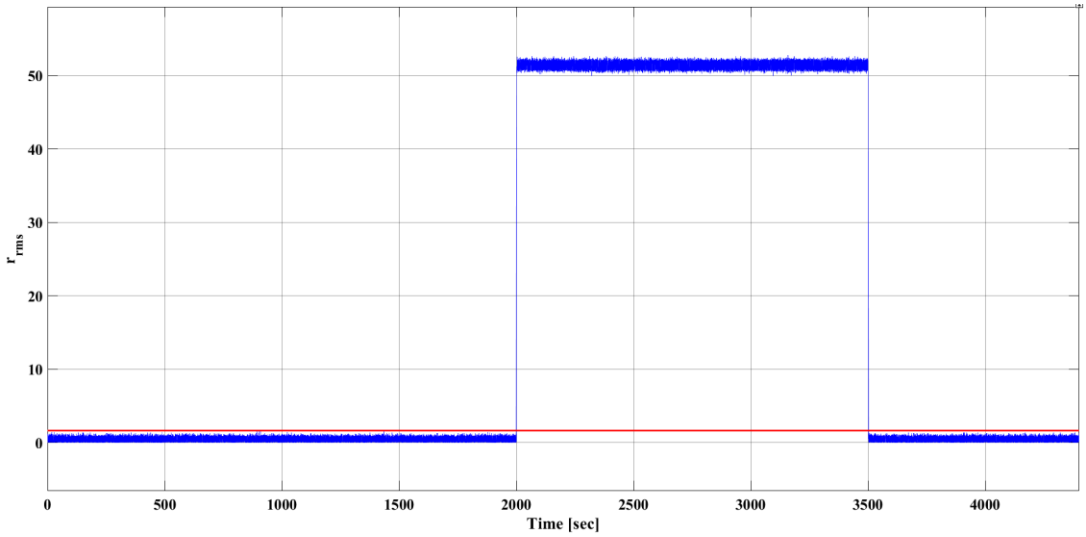

Figure 5.4: Residual value during fault 3 occurrence (when β_1 is faulty).

Figure 5.5 show the residual value during fault 4 occurrence (when β_2 is faulty). The residual value is more than 60 times of threshold value, i.e., easy and direct fault detection.

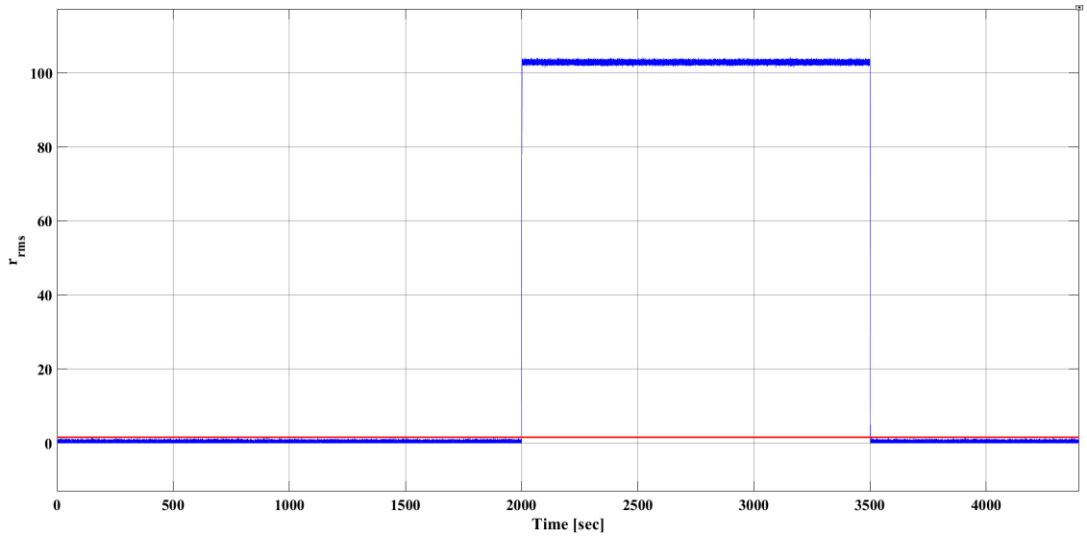

Figure 5.5: Residual value during fault 4 occurrence (when β_2 is faulty).

Figure 5.6 show the residual value during fault 5 occurrence (when β_3 is faulty). The residual value is about 100 times of threshold value, i.e., easy and direct fault detection.

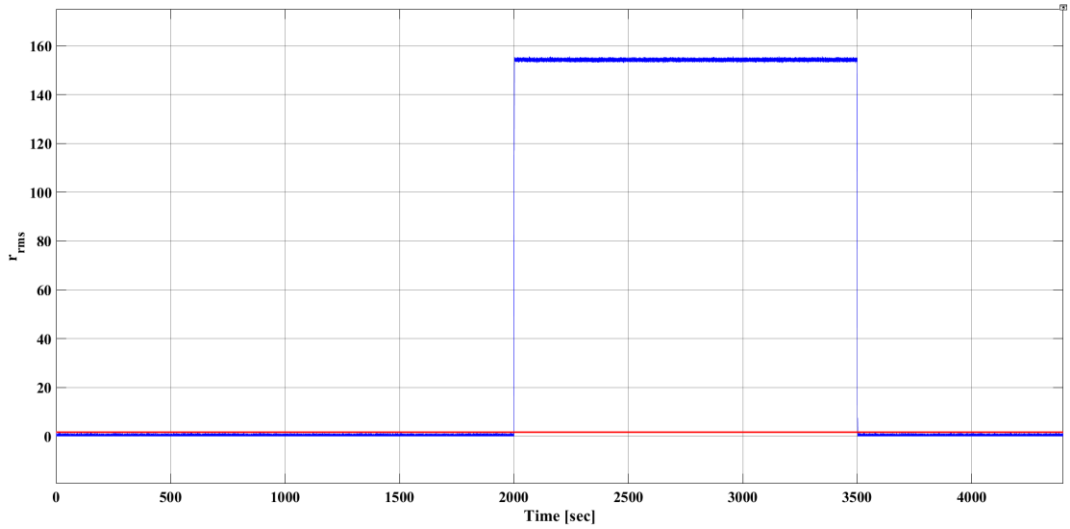

Figure 5.6: Residual value during fault 5 occurrence (when β_3 is faulty).

Figure 5.7 shows the speed of fault detection for faulty generator speed measurement (fault occurs at 2000 sec. and detected at 2000.05 sec.) The speed of fault detection for generator speed measurement, rotor speed measurement, and pitch angle faults was 47-51 msec. This high speed of fault detection gives the proposed scheme the power of the online quick reaction for any sensor fault under consideration.

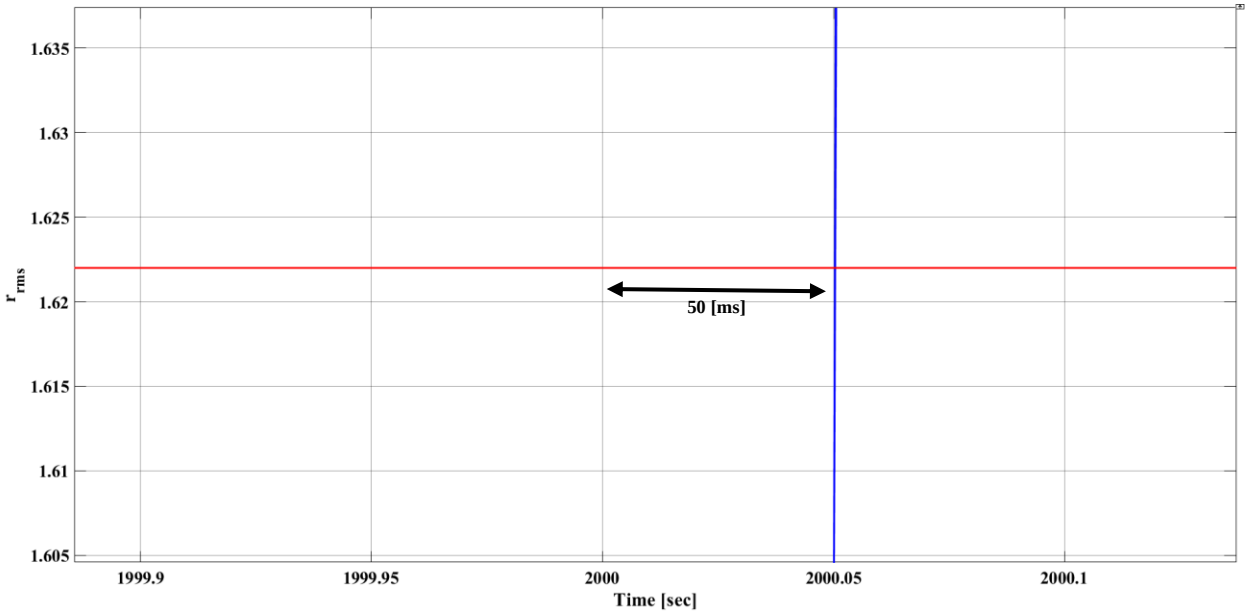

Figure 5.7: Fault detection rate.

5.3 AFTC Algorithm

Figure 5.8 shows the proposed AFTC algorithm structure, which is the main contribution of this thesis. The algorithm shows how to isolate and reconstruct the faulty sensor signals in real time simply, effectively, and within few seconds. Both of the real sensor measurements and the accommodated ones are considered by the actions of the AFTC Algorithm. The accommodated measurements resources are from the same turbine's sensors with predefined built-in computation, or from the corresponding sensors of other turbines that are in the same wind farm zone.

The supervisory block compares the two measurements to detect the fault and isolate the faulty sensors. In matter fact, the wind turbine is maintained in a continuous correct operation whenever a fault is detected by the adoption of the reconstructed signals by the supervisory block. The AFTC algorithm steps can be summarized as follows:

AFTC Steps
• Step 1: Evaluate the residual signal based on (5.3). • Step 2: Detect the fault based on (5.5) and the decision logic.

- Step 3: Estimate the accommodated signal using other sensors' measurements of the same wind turbine if possible, or using the corresponding sensors' measurements of the near turbine in the same zone of the wind farm.
- Step 4: If no fault is detected, then sensors measurements will be fed back to the closed-loop controller.
- Step 5: If a fault is detected in any sensor measurements, then an accommodated corresponding signal will be sent instead of the faulty signal.
- Step 6: Send a faulty-sensor alarm signal to the monitoring system.

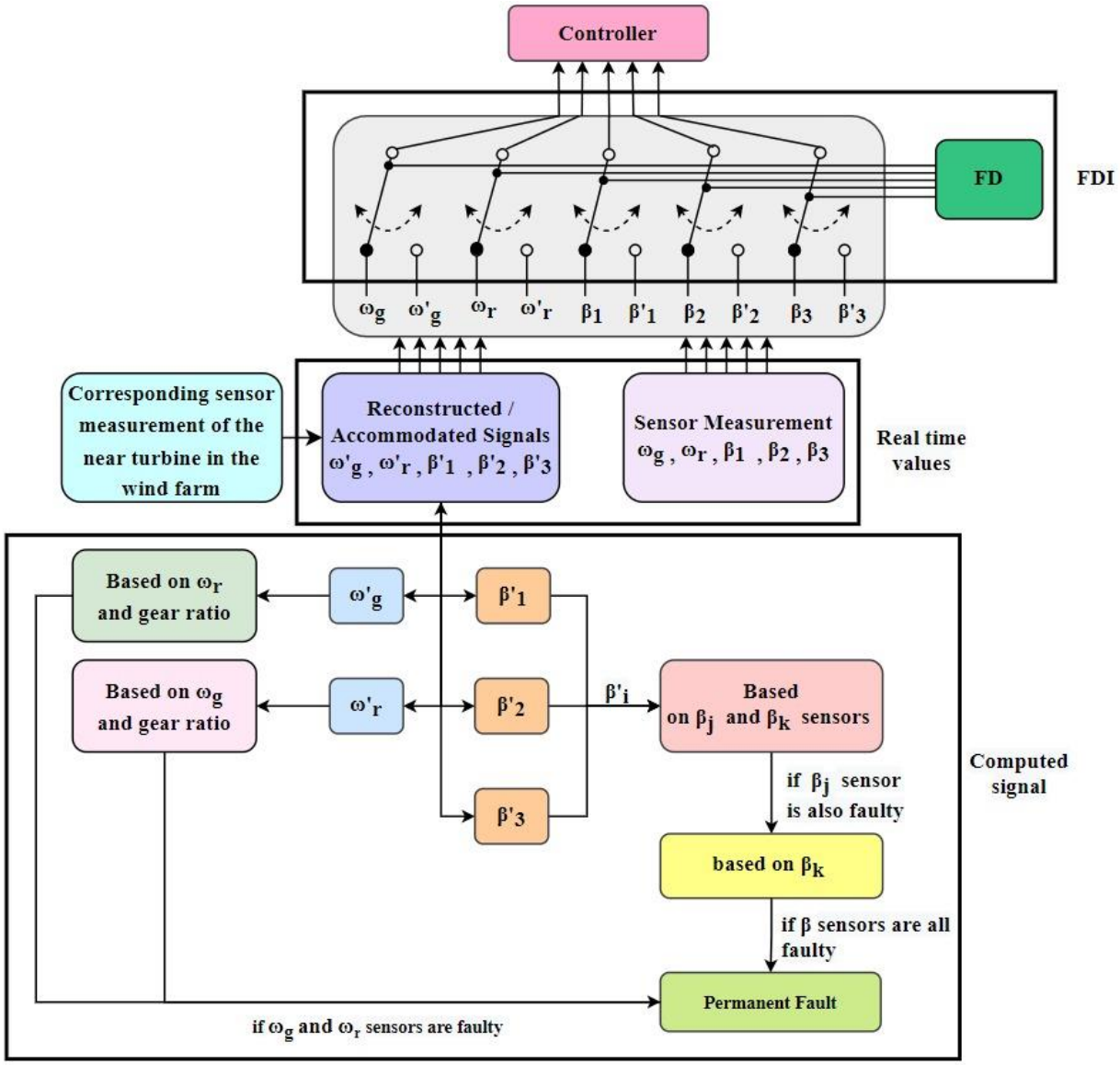

Figure 5.8: AFTC Algorithm Structure.

A. AFTC Algorithm Testing

The proposed algorithm was tested using MATLAB/Simulink Benchmark model. Figure 5.9 shows the corresponding speed sensor measurement of the near turbine in the wind farm, which is assumed to be 50 rpm lower due to differences in mechanical parts between the identical turbines. The resulting effects on the generated power was slight compared with the fault-free operation mode as shown in figure 5.10.

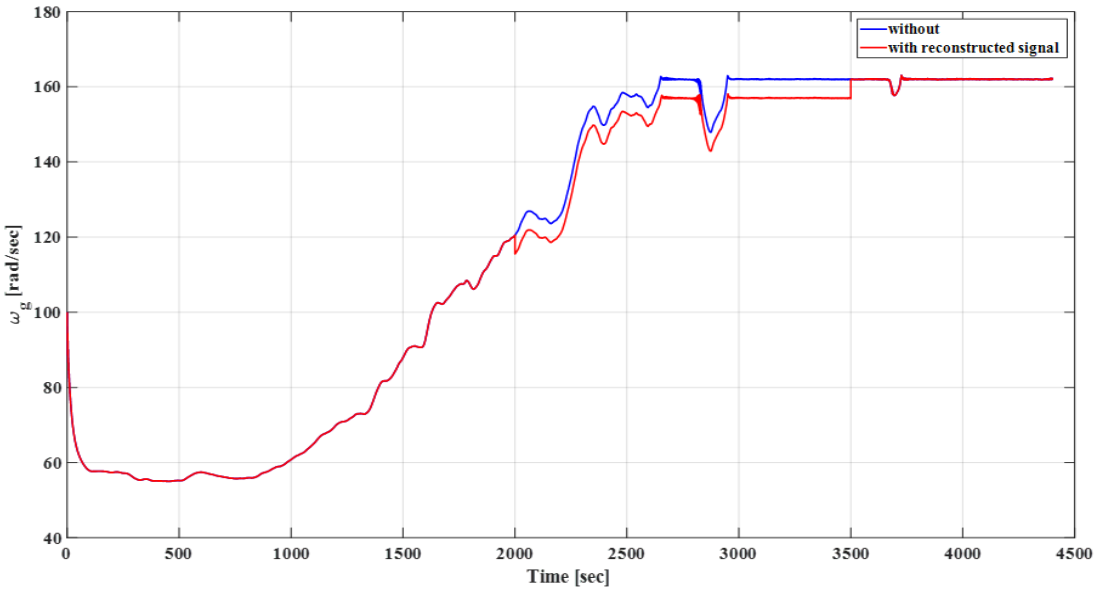

Figure 5.9: Corresponding ω_g sensor measurement of the near turbine in the wind farm

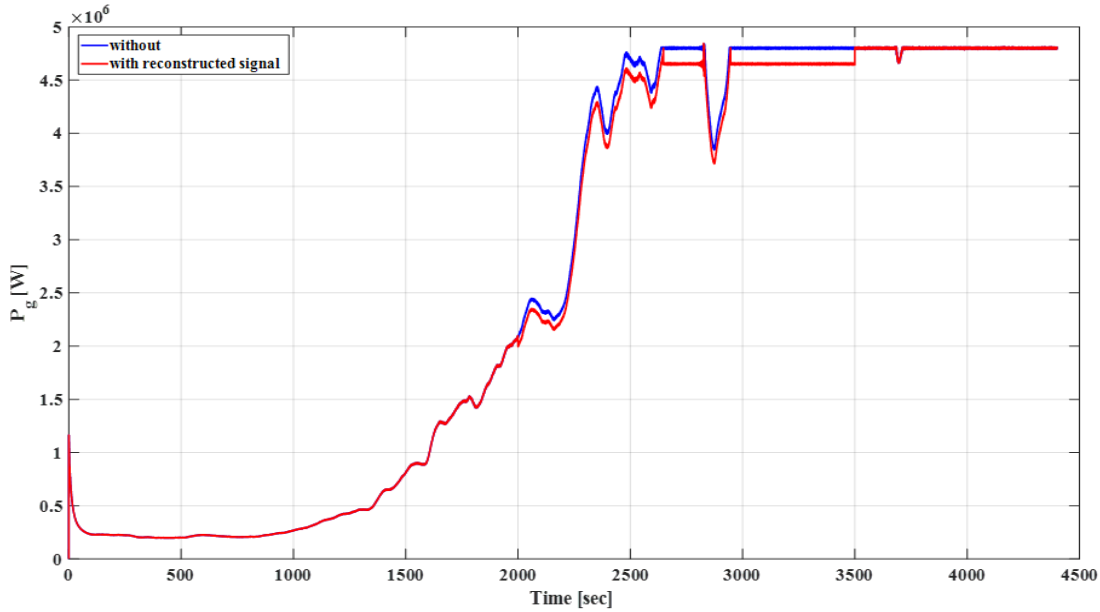

Figure 5.10: P_g measurement using reconstructed signal of ω_g.

B. Technical Applicability

Any type of controller could be used like PLC with high-speed processor and clocking speed and as many as required analog inputs to read the field devices like speed sensors and power measuring devices in addition to a communication module to support any field bus protocol used in the site such as Modbus or TCP/IP Ethernet protocol to communicate the data with other controllers and also with the site operators if valid through HMI or local PC. The processed data can be monitored remotely through any type of gateway, such as a web-embedded server gateway to let the remote operator.

To monitor or even to control the system if required from anywhere. The sampling rate's low frequency of 100 Hz allows all previously mentioned devices to process and transmit the data within the time limits.

So, regarding the online capability of the controller, it is so clear that it is easily affordable on-site, but remotely, it will be limited to the communication media speed. Also, the plc and the gateway have the logging capability with time stamping to facilitate the fault isolation process.

Chapter Six

Conclusion and Future Work

6.1 Conclusion

Sensors faults in pitch angles positions, rotor and generator speeds were investigated, each fault effects on wind turbine performance were studied. It was noticed that the effects of the aforementioned sensors' faults on wind turbine performance were significantly high.

A fault detection filter has been formulated and adopted to the wind turbine model. The sensor fault detection process has been tested on the wind turbine benchmark model. The investigated sensor faults were all detected successfully by the adopted detection filter.

An algorithm was developed to overcome the missing measurement signals of the sensors and provide the controller with alternative solutions so the turbine can continue the operation with high performance, reliability, and safety.

6.2 Recommended Future Work

Researchers interested in this topic can invest in this research and build on it to include other types of faults, especially actuator faults. It is also possible to investigate optimization techniques for the fault detection process, which will help reduce the impact of disturbances and increase faults sensitivity while focusing on the need to reduce the complexity of the computational process to maintain a fast fault detection rate.

Bibliography

[1] S. Simani, "Overview of Modelling and Advanced Control Strategies for Wind Turbine Systems," *Energies*, vol. 8, no. 12, pp. 13395–13418, Dec. 2015

[2] F. Shi and R. Patton, "An active fault tolerant control approach to an offshore wind turbine model," *Renewable Energy*, vol. 75, pp. 788–798, Mar. 2015

[3] D. R. Media, "Global Wind Power Back on Track," Global Wind Energy Council, Feb. 10, 2015. https://gwec.net/global-wind-power-back-track.

[4] M. J. Kabir, A. M. T. Oo, and M. Rabbani, "A brief review on offshore wind turbine fault detection and recent development in condition monitoring based maintenance system," in *2015 Australasian Universities Power Engineering Conference (AUPEC)*, Sep. 2015, pp. 1–7.

[5] B. Knopf, P. Nahmmacher, and E. Schmid, "The European renewable energy target for 2030 – An impact assessment of the electricity sector," *Energy Policy*, vol. 85, no. C, pp. 50–60, 2015.

[6] "Danmark sætter ny rekord i vind," Dansk Energi. https://www.danskenergi.dk/nyheder/danmark-saetter-ny-rekord-vind (accessed Nov. 07, 2021).

[7] X. Wei, M. Verhaegen, and T. van den Engelen, "Sensor Fault Diagnosis of Wind Turbines for Fault Tolerant," *IFAC Proceedings Volumes*, vol. 41, no. 2, pp. 3222–3227, Jan. 2008

[8] Z. Feng, M. Liang, Y. Zhang, and S. Hou, "Fault diagnosis for wind turbine planetary gearboxes via demodulation analysis based on ensemble empirical mode decomposition and energy separation," *Renewable energy*, 2012

[9] D. McMillan and G. W. Ault, "Quantification of Condition Monitoring Benefit for Offshore Wind Turbines," *Wind Engineering*, vol. 31, no. 4, pp. 267–285, May 2007

[10] C. A. Walford, "Wind turbine reliability :understanding and minimizing wind turbine operation and maintenance costs.," Sandia National Laboratories (SNL), Albuquerque, NM, and Livermore, CA (United States), SAND2006-1100, Mar. 2006

[11] S. Simani, S. Farsoni, and P. Castaldi, "Fault Diagnosis of a Wind Turbine Benchmark via Identified Fuzzy Models," IEEE Transactions on Industrial Electronics, vol. 62, no. 6, pp. 3775–3782, Jun. 2015

[12] Y. Feng, P. J. Tavner, and H. Long, "Early experiences with UK Round 1 offshore wind farms.," Proceedings of the Institution of Civil Engineers : energy., vol. 163, no. 4, pp. 167–181, Nov. 2010

[13] M. Entezami, S. Hillmansen, P. Weston, and M. P. Papaelias, “Fault detection and diagnosis within a wind turbine mechanical braking system using condition monitoring,” Renewable Energy, vol. 47, no. C, pp. 175–182, 2012.

[14] P. F. Odgaard, J. Stoustrup, and M. Kinnaert, “Fault Tolerant Control of Wind Turbines – a benchmark model,” IFAC Proceedings Volumes, vol. 42, no. 8, pp. 155–160, Jan. 2009

[15] Z. Hameed, Y. S. Hong, Y. M. Cho, S. H. Ahn, and C. K. Song, “Condition monitoring and fault detection of wind turbines and related algorithms: A review,” Renewable and Sustainable Energy Reviews, vol. 13, no. 1, pp. 1–39, 2009.

[16] G. de N. P. Leite, A. M. Araújo, and P. A. C. Rosas, “Prognostic techniques applied to maintenance of wind turbines: a concise and specific review,” Renewable and Sustainable Energy Reviews, vol. 81, no. P2, pp. 1917–1925, 2018.

[17] H. Habibi, I. Howard, and S. Simani, “Reliability improvement of wind turbine power generation using model-based fault detection and fault tolerant control: A review,” Renewable Energy, vol. 135, pp. 877–896, May 2019

[18] P. F. Odgaard, J. Stoustrup, and M. Kinnaert, “Fault-Tolerant Control of Wind Turbines: A Benchmark Model,” IEEE Transactions on Control Systems Technology, vol. 21, no. 4, pp. 1168–1182, Jul. 2013

[19] H. Alwi, C. Edwards, and C. P. Tan, “Fault Tolerant Control and Fault Detection and Isolation,” in Fault Detection and Fault-Tolerant Control Using Sliding Modes, H. Alwi, C. Edwards, and C. Pin Tan, Eds. London: Springer, 2011, pp. 7–27. doi: 10.1007/978-0-85729-650-4_2.

[20] “Fault Diagnosis and Fault-Tolerant Control of Wind Turbines - Project Library, Aalborg University.” https://projekter.aau.dk/projekter/en/studentthesis/fault-diagnosis-and-faulttolerant-control-of-wind-turbines(03701c79-ce36-4e20-ae03-806704080be9).html?fbclid=IwAR31EzbwqtFWptNeWMfwtSA-bv9dt78RasLXlEhI6_ouyk7wDA3yTGnv57U .

[21] H. Niemann and J. Stoustrup, “Passive fault tolerant control of a double inverted pendulum—a case study,” Control Engineering Practice, vol. 13, no. 8, pp. 1047–1059, Aug. 2005, doi: 10.1016/j.conengprac.2004.11.002.

[22] A. A. Amin and K. M. Hasan, “A review of Fault Tolerant Control Systems: Advancements and applications,” Measurements, vol. 143, pp. 58–68, Sep. 2019

[23] R. Isermann and P. Ballé, “Trends in the application of model-based fault detection and diagnosis of technical processes,” Control Engineering Practice, vol. 5, no. 5, pp. 709–719, May 1997

[24] J. Chen and R. J. Patton, “Basic Principles of Model-Based Fault Diagnosis,” in Robust Model-Based Fault Diagnosis for Dynamic Systems, J. Chen and R. J. Patton, Eds. Boston, MA: Springer US, 1999, pp. 19–64. doi: 10.1007/978-1-4615-5149-2_2.

[25] R. Isermann, “Process fault detection based on modeling and estimation methods—A survey,” Automatica, vol. 20, no. 4, pp. 387–404, Jul. 1984

[26] M. Saif and Y. Guan, “A new approach to robust fault detection and identification,” IEEE Transactions on Aerospace and Electronic Systems, vol. 29, no. 3, pp. 685–695, Jul. 1993, doi: 10.1109/7.220921.

[27] C. Edwards and S. K. Spurgeon, Sliding mode control: theory and applications. London: Taylor & Francis, 1998.

[28] C. Edwards, S. K. Spurgeon, and R. J. Patton, “Sliding mode observers for fault detection and isolation,” Automatica, vol. 36, no. 4, pp. 541–553, Apr. 2000, doi: 10.1016/S0005-1098(99)00177-6.

[29] C. P. Tan and C. Edwards, “Sliding mode observers for robust detection and reconstruction of actuator and sensor faults,” International Journal of Robust and Nonlinear Control, vol. 13, no. 5, pp. 443–463, 2003, doi: 10.1002/rnc.723.

[30] V. I. Utkin, “State Observation and Filtering,” in Sliding Modes in Control and Optimization, V. I. Utkin, Ed. Berlin, Heidelberg: Springer, 1992, pp. 206–222. doi: 10.1007/978-3-642-84379-2_14.

[31] P. Gerland, D. Groß, H. Schulte, and A. Kroll, “Design of sliding mode observers for TS fuzzy systems with application to disturbance and actuator fault estimation,” in 49th IEEE Conference on Decision and Control (CDC), Dec. 2010, pp. 4373–4378. doi: 10.1109/CDC.2010.5717065.

[32] S. Georg and H. Schulte, “Takagi-Sugeno Sliding Mode Observer with a Weighted Switching Action and Application to Fault Diagnosis for Wind Turbines,” in Intelligent Systems in Technical and Medical Diagnostics, Berlin, Heidelberg, 2014, pp. 41–52. doi: 10.1007/978-3-642-39881-0_3.

[33] R. J. Patton, “Fault-Tolerant Control: The 1997 Situation,” IFAC Proceedings Volumes, vol. 30, no. 18, pp. 1029–1051, Aug. 1997

[34] N. Laouti, N. Sheibat-Othman, and S. Othman, “Support Vector Machines for Fault Detection in Wind Turbines,” IFAC Proceedings Volumes, vol. 44, no. 1, pp. 7067–7072, Jan. 2011

[35] X. Zhang, Q. Zhang, S. Zhao, R. Ferrari, M. M. Polycarpou, and T. Parisini, “Fault Detection and Isolation of the Wind Turbine Benchmark: an Estimation-based Approach,” IFAC Proceedings Volumes, vol. 44, no. 1, pp. 8295–8300, Jan. 2011

[36] F. D. Bianchi, R. J. Mantz, and H. De Battista, Eds., “Control of Variable-speed Variable-pitch Wind Turbines Using Gain Scheduling Techniques,” in Wind Turbine Control Systems: Principles, Modelling and Gain Scheduling Design, London: Springer, 2007, pp. 115–149. doi: 10.1007/1-84628-493-7_6.

[37] “The Controller,” in Wind Energy Handbook, John Wiley & Sons, Ltd, pp. 475–523. doi: 10.1002/9781119992714.ch8.

[38] K. E. Johnson, L. Y. Pao, M. J. Balas, and L. J. Fingersh, “Control of variable-speed wind turbines: standard and adaptive techniques for maximizing energy capture,” IEEE Control Systems Magazine, vol. 26, no. 3, pp. 70–81, Jun. 2006

[39] P. F. Odgaard and J. Stoustrup, “Fault tolerant wind farm control — A benchmark model,” in 2013 IEEE International Conference on Control Applications (CCA), Aug. 2013, pp. 412–417. doi: 10.1109/CCA.2013.6662784.

[40] D. van Schrick, “Remarks on Terminology in the Field of Supervision, Fault Detection and Diagnosis,” IFAC Proceedings Volumes, vol. 30, no. 18, pp. 959–964, Aug. 1997

[41] E. Kamal and A. Aitouche, “Robust fault tolerant control of DFIG wind energy systems with unknown inputs,” Renewable Energy, vol. 56, pp. 2–15, Aug. 2013

[42] H. Tohidi, K. Erenturk, and S. Shoja-Majidabad, “Passive Fault Tolerant Control of Induction Motors Using NBC,” Journal of Control Engineering and Applied Informatics, vol. 19, no. 1, pp. 49–58, Mar. 2017.

[43] Y. Zhang and J. Jiang, “Bibliographical review on reconfigurable fault-tolerant control systems,” IFAC Proceedings Volumes, vol. 36, no. 5, pp. 257–268, Jun. 2003, doi: 10.1016/S1474-6670(17)36503-5.

[44] F. Liao, J. L. Wang, and G.-H. Yang, “Reliable H/sub 2/ static output-feedback tracking control against aircraft wing/control surface impairment,” in 2003 IEEE International Workshop on Workload Characterization (IEEE Cat. No.03EX775), Aug. 2003, vol. 1, pp. 112–117 vol.1. doi: 10.1109/PHYCON.2003.1236798.

[45] Z. Hameed, Y. S. Hong, Y. M. Cho, S. H. Ahn, and C. K. Song, “Condition monitoring and fault detection of wind turbines and related algorithms: A review,” Renewable and Sustainable Energy Reviews, vol. 13, no. 1, pp. 1–39, 2009.

[46] X. Wei and M. Verhaegen, “Fault detection of large scale wind turbine systems: A mixed H∞/H− index observer approach,” in 2008 16th Mediterranean Conference on Control and Automation, Jun. 2008, pp. 1675–1680. doi: 10.1109/MED.2008.4601998.

[47] S. S. Donders, “Fault Detection and Identification for Wind Turbine Systems: a closed-loop analysis,” Master’s Thesis, University of Twente Faculty of Applied Physics Systems and Control Engineering, 2002. [Online]. Available: http://www.stijndonders.nl/wind/scriptie.pdf

[48] A. Mouzakitis, “Classification of Fault Diagnosis Methods for Control Systems,” Measurement and Control, vol. 46, no. 10, pp. 303–308, Dec. 2013

[49] I. Hwang, S. Kim, Y. Kim, and C. E. Seah, “A Survey of Fault Detection, Isolation, and Reconfiguration Methods,” IEEE Transactions on Control Systems Technology, vol. 18, no. 3, pp. 636–653, May 2010, doi: 10.1109/TCST.2009.2026285.

[50] K. E. Johnson and P. A. Fleming, “Development, implementation, and testing of fault detection strategies on the National Wind Technology Center’s controls advanced research turbines,” Mechatronics, vol. 21, no. 4, pp. 728–736, Jun. 2011, doi: 10.1016/j.mechatronics.2010.11.010.

[51] R. V. Beard, “Failure accomodation in linear systems through self-reorganization.,” Thesis, Massachusetts Institute of Technology, 1971

[52] H. L. Jones, “Failure detection in linear systems.,” Thesis, Massachusetts Institute of Technology, 1973.

[53] J. White and J. Speyer, “Detection filter design: Spectral theory and algorithms,” IEEE Transactions on Automatic Control, vol. 32, no. 7, pp. 593–603, Jul. 1987, doi: 10.1109/TAC.1987.1104682.

[54] J. PARK and G. RIZZONI, “A new interpretation of the fault detection filter Part 1: Closed-form algorithm,” International Journal of Control, vol. 60, no. 5, pp. 767–787, Nov. 1994, doi: 10.1080/00207179408921494.

[55] J. PARK, Y. HALEVI, and G. RIZZONI, “A new interpretation of the fault-detection filter Part 2. The optimal detection filter,” International Journal of Control, vol. 60, no. 6, pp. 1339–1351, Dec. 1994, doi: 10.1080/00207179408921525.

[56] R. N. Clark, D. C. Fosth, and V. M. Walton, “Detecting Instrument Malfunctions in Control Systems,” IEEE Transactions on Aerospace and Electronic Systems, vol. AES-11, no. 4, pp. 465–473, Jul. 1975, doi: 10.1109/TAES.1975.308108.

[57] J. Wünnenberg and P. M. Frank, “Sensor Fault Detection via Robust Observers,” in System Fault Diagnostics, Reliability and Related Knowledge-Based Approaches, Dordrecht, 1987, pp. 147–160. doi: 10.1007/978-94-009-3929-5_5.

[58] J. Deckert, M. Desai, J. Deyst, and A. Willsky, “F-8 DFBW sensor failure identification using analytic redundancy,” IEEE Transactions on Automatic Control, vol. 22, no. 5, pp. 795–803, Oct. 1977, doi: 10.1109/TAC.1977.1101598.

[59] J. Gertler, “Fault detection and isolation using parity relations,” Control Engineering Practice, vol. 5, no. 5, pp. 653–661, May 1997, doi: 10.1016/S0967-0661(97)00047-6.

[60] C. Baskiotis, J. Raymond, and A. Rault, “Parameter identification and discriminant analysis for jet engine machanical state diagnosis,” in 1979 18th IEEE Conference on Decision and Control including the Symposium on Adaptive Processes, Dec. 1979, vol. 2, pp. 648–650. doi: 10.1109/CDC.1979.270264.

[61] R. Isermann, “Process fault detection based on modeling and estimation methods—A survey,” Automatica, vol. 20, no. 4, pp. 387–404, Jul. 1984, doi: 10.1016/0005-1098(84)90098-0.

[62] R. K. Mehra and J. Peschon, “An innovations approach to fault detection and diagnosis in dynamic systems,” Automatica, vol. 7, no. 5, pp. 637–640, Sep. 1971, doi: 10.1016/0005-1098(71)90028-8.

[63] A. S. Willsky, “A survey of design methods for failure detection in dynamic systems,” Automatica, vol. 12, no. 6, pp. 601–611, Nov. 1976, doi: 10.1016/0005-1098(76)90041-8.

[64] M. Basseville, “Detecting changes in signals and systems—A survey,” Automatica, vol. 24, no. 3, pp. 309–326, May 1988, doi: 10.1016/0005-1098(88)90073-8.

[65] Michèle Basseville, Igor Nikiforov. Detection of Abrupt Changes - Theory and Application. Prentice Hall, Inc. - http://people.irisa.fr/Michele.Basseville/kniga/, pp.550, 1993. ⟨hal-00008518⟩

[66] R. J. Patton and J. Chen, “Robust fault detection using eigenstructure assignment: a tutorial consideration and some new results,” in [1991] Proceedings of the 30th IEEE Conference on Decision and Control, Dec. 1991, pp. 2242–2247 vol.3. doi: 10.1109/CDC.1991.261546.

[67] R. J. Patton and J. Chen, “Review of parity space approaches to fault diagnosis for aerospace systems,” Journal of Guidance, Control, and Dynamics, vol. 17, no. 2, pp. 278–285, Mar. 1994, doi: 10.2514/3.21194.

[68] Gertler, J.J. (1998). Fault Detection and Diagnosis in Engineering Systems (1st ed.). CRC Press. https://doi.org/10.1201/9780203756126

[69] J. Chen and R. J. Patton, “Basic Principles of Model-Based Fault Diagnosis,” in Robust Model-Based Fault Diagnosis for Dynamic Systems, J. Chen and R. J. Patton, Eds. Boston, MA: Springer US, 1999, pp. 19–64. doi: 10.1007/978-1-4615-5149-2_2.

[70] “On-line Approaches,” in Adaptive Filtering and Change Detection, John Wiley & Sons, Ltd, pp. 55–87. doi: 10.1002/0470841613.ch3.

[71] Z. Kowalczuk and P. Suchomski, “Control Theory Methods in Designing Diagnostic Systems,” in Fault Diagnosis: Models, Artificial Intelligence, Applications, J. Korbicz, Z. Kowalczuk, J. M. Kościelny, and W. Cholewa, Eds. Berlin, Heidelberg: Springer, 2004, pp. 155–218. doi: 10.1007/978-3-642-18615-8_5.

[72] V. Venkatasubramanian, R. Rengaswamy, K. Yin, and S. N. Kavuri, “A review of process fault detection and diagnosis: Part I: Quantitative model-based methods,” Computers & Chemical Engineering, vol. 27, no. 3, pp. 293–311, Mar. 2003, doi: 10.1016/S0098-1354(02)00160-6.

[73] V. Venkatasubramanian, R. Rengaswamy, and S. N. Kavuri, “A review of process fault detection and diagnosis: Part II: Qualitative models and search strategies,” Computers & Chemical Engineering, vol. 27, no. 3, pp. 313–326, Mar. 2003, doi: 10.1016/S0098-1354(02)00161-8.

[74] V. Venkatasubramanian, R. Rengaswamy, S. N. Kavuri, and K. Yin, “A review of process fault detection and diagnosis: Part III: Process history based methods,” Computers & Chemical Engineering, vol. 27, no. 3, pp. 327–346, Mar. 2003, doi: 10.1016/S0098-1354(02)00162-X.

[75] C. Angeli and A. Chatzinikolaou, “On-line Fault Detection Techniques for Technical Systems: A survey,” International Journal of Computer Science & Applications, Vol, vol. 1, no. 1, pp. 12–30, 2004.

[76] R. Isermann, “Model-based fault-detection and diagnosis – status and applications,” Annual Reviews in Control, vol. 29, no. 1, pp. 71–85, Jan. 2005, doi: 10.1016/j.arcontrol.2004.12.002.

[77] K. Xiahou, Y. Liu, L. Wang, M. S. Li and Q. H. Wu, "Switching Fault-Tolerant Control for DFIG-Based Wind Turbines With Rotor and Stator Current Sensor Faults," in IEEE Access, vol. 7, pp. 103390-103403, 2019, doi: 10.1109/ACCESS.2019.2931927.

[78] H. Badihi, S. Jadidi, Y. Zhang, P. Pillay and S. Rakheja, "Fault-Tolerant Cooperative Control in a Wind Farm Using Adaptive Control Reconfiguration and Control Reallocation," in IEEE Transactions on Sustainable Energy, vol. 11, no. 4, pp. 2119-2129, Oct. 2020, doi: 10.1109/TSTE.2019.2950681

[79] T. Jain and J. J. Yamé, "Fault-Tolerant Economic Model Predictive Control for Wind Turbines," in IEEE Transactions on Sustainable Energy, vol. 10, no. 4, pp. 1696-1704, Oct. 2019, doi: 10.1109/TSTE.2018.2869480

[80] H. Badihi, Y. Zhang, P. Pillay and S. Rakheja, "Fault-Tolerant Individual Pitch Control for Load Mitigation in Wind Turbines With Actuator Faults," in IEEE Transactions on Industrial Electronics, vol. 68, no. 1, pp. 532-543, Jan. 2021, doi: 10.1109/TIE.2020.2965479

[81] H. Habibi, I. Howard, S. Simani and A. Fekih, "Decoupling Adaptive Sliding Mode Observer Design for Wind Turbines Subject to Simultaneous Faults in Sensors and Actuators," in IEEE/CAA Journal of Automatica Sinica, vol. 8, no. 4, pp. 837-847, April 2021, doi: 10.1109/JAS.2021.1003931

[82] R. K. Douglas and J. L. Speyer, “Robust fault detection filter design,” Journal of Guidance, Control, and Dynamics, vol. 19, no. 1, pp. 214–218, 1996, doi: 10.2514/3.21600.

[83] “Danish Wind Turbines: An Industrial Success Story.” http://ele.aut.ac.ir/~wind/en/articles/success.htm

[84] H. Badihi, Y. Zhang, and H. Hong, “Fault-Tolerant Control design for a large off-shore wind turbine using Fuzzy Gain-Scheduling and Signal Correction,” in 2013 American Control Conference, Jun. 2013, pp. 1448–1453. doi: 10.1109/ACC.2013.6580040.

[85] X. Yang and J. M. Maciejowski, “Fault-tolerant model predictive control of a wind turbine benchmark,” IFAC Proceedings Volumes, vol. 45, no. 20, pp. 337–342, Jan. 2012, doi: 10.3182/20120829-3-MX-2028.00134.

[86] S. Georg, “Fehlerdiagnose und Fehlertolerante Regelung von WindenergieanlagenFault diagnosis and fault-tolerant control of wind turbines,” 2015, doi: 10.18453/ROSDOK_ID00001468.

[87] “Ali Abdo - Fault Detection Schemes for Switched Systems.” http://www.shaker.de/de/content/catalogue/index.asp?lang=de&ID=8&ISBN=978-3-8440-2234-6.

[88] S. X. Ding, Model-Based Fault Diagnosis Techniques: Design. Schemes Algorithms, and Tools, 2nd ed. Berlin, Germany: Springer,. 2013